(NASA-CR-163194) EFFECTS OF FREE-STREAM TURBULENCE ON DIFFUSER PERFORMANCE (California Polytechnic State Univ.) 51 p HC A04/MF A01 CSCL 01A

N80-24264

Unclas
G3/02 20979

Effects of Free-Stream Turbulence On Diffuser Performance

(Prepared under NASA-ARC Grant #NSG-2391)

By

Jon A. Hoffmann, Professor
Aeronautical Engineering Department
California Polytechnic State University
San Luis Obispo, CA 93407

June, 1980

ABSTRACT

An experimental evaluation of the effects of free-stream turbulence on the performance of a subsonic two-dimensional diffuser has been made. Increases of the diffuser's static pressure recovery coefficient of 11.4 and 21.1 percent at total included divergence angles of 12 and 20 degrees respectively were obtained when the value of the inlet integral free-stream scale of turbulence in the flow direction was at least 7.5 times larger than the inlet boundary layer displacement thickness, and when the inlet total free-stream turbulence intensity was at least 3.5 percent. It is hypothesized that a larger scale of turbulence transmits the free-stream energy to the wall more effectively and when coupled with large turbulence intensities, are mechanisms which act to decrease the distortion and delay separation within the diffuser.

NOMENCLATURE

AR = diffuser area ratio, W_2/W_1

b = distance between parallel walls of diffuser

b_o = rod length

c = channel length

C_p = static pressure recovery coefficient, $(P_2-P_1)/\rho \bar{U}^2/2$

C_o = pressure loss coefficient across rods, $\Delta P_o/\rho \bar{U}^2/2$

D = rod diameter

$f(\omega)$ = fraction of turbulent energy in flow direction contained between frequency ω and $\omega+d\omega$

H = shape factor, δ^*/δ^{**}

L = diffuser wall length

n = number of rods

N = diffuser axial length

P = static pressure

$\sqrt{\overline{q'^2}}$ = total RMS Turbulence Intensity, $\sqrt{(\overline{u'^2} + \overline{v'^2} + \overline{w'^2})/3}$

r = radius of rod set geometry

R_e = Reynolds number, $\bar{U}W_1/\nu$

R_x = free-stream autocorrelation coefficient in flow direction at diffuser inlet,

$$\overline{u'(x)\, u'(x - \Delta x)} \;/\; \overline{u'^2}$$

R_y = free-stream crosscorrelation coefficient in y direction at diffuser inlet,

$$\overline{u'(y)\, u'(y - \Delta y)} \;/\; \overline{u'^2}$$

S = throat section dimension (see figure 2)

t = time

$\bar{u}$ = average velocity in flow direction at diffuser inlet

u' = turbulence component in flow direction at diffuser inlet

$\bar{U}$ = mass average velocity at diffuser inlet

U_m = average free-stream velocity in flow direction at diffuser inlet

v' = turbulence component in y direction at diffuser inlet

W = diffuser width measured between diverging walls

w' = turbulence component in z direction at diffuser inlet

δ^* = boundary layer displacement thickness at diffuser inlet

δ^{**} = boundary layer momentum thickness at diffuser inlet

θ = divergence angle of diffuser wall

ν = kinematic viscosity

λ_x = free-stream scale of turbulence at diffuser inlet in x direction,

$$\int_0^\infty R_x \, dx$$

λ_y = free-stream scale of turbulence at diffuser inlet in y direction,

$$\int_0^\infty R_y \, dy$$

ρ = fluid density

ω = frequency, H_z

Subscripts

0 = location of rods

1 = diffuser inlet ($0.49W_1$ upstream from beginning of diffuser wall curvature)

2 = diffuser exit

x = flow direction

y = direction normal to the flow and parallel to the parallel walls of the diffuser

z = direction normal to the flow and perpendicular to the parallel walls of the diffuser

TABLE OF CONTENTS

LIST OF FIGURES

INTRODUCTION

A diffuser, one of the basic components of systems utilizing fluid flow, is a device in which the inlet dynamic pressure of a fluid is converted to a static pressure rise. For subsonic flow, this is done by decelerating the fluid by means of a gradual increase of the cross sectional flow area. It is desirable to recover as large a part of the entering dynamic pressure as possible; also, the exiting flow should be as steady as possible. An understanding of the basic mechanisms which control diffuser performance will lead to the design of systems which employ techniques to utilize these mechanisms in improving the efficiency of fluid machines.

The literature contains many studies of diffuser performance such as those presented by Cockrell (1), McDonald (2) and Sovran (3). Early studies of the behavior of a diffuser's internal flow were performed by Moore and Kline (4) and Fox and Kline (5). They found the existence of four operational zones of a diffuser with a constant ratio of length to throat width. These are: first, a zone of no appreciable stall or separation at the smallest divergence angles; second, a zone of unsteady flow with three-dimensional transitory separation; third, a zone of steady, very stable, two-dimensional separation at large divergence angles; and fourth, a zone of two-dimensional jet separation at very large divergence angles.

The transitory stall regime was further investigated by Smith and Kline (6). Their experiments were done with both undisturbed and periodically disturbed conditions. One of their significant accomplishments was that, for the undisturbed inlet condition, the measure washout period was found to be proportional to the diffuser length and the included angle, and inversely proportional to the area averaged inlet velocity. Washout is defined in their report as a rapid entrainment and expulsion of a stall from the diffuser by the through flow. For the

periodically disturbed inlet condition, they succeeded in triggering the washout entirely by the pulsed disturbances, where the pulse period ranged from 0.5 to 1.0 times the mean washout period. This result may be applied in regulating transitory stall, and may be the beginning of a controlled stall study.

Up to the present time, various methods of increasing the pressure recovery of diffusers have been investigated. When Moore and Kline (4) place one rod ($D/W_1 = 1.25$) at the lip of the diffuser entrance with $2\theta = 45^{o}$, the existing stall was eliminated, and the pressure recovery coefficient increased from 0.3 to 0.575. It was hypothesized that the rod generated its own vortices which in turn increased the turbulence level, and thereby improved the performance of the diffuser. Also, Waitman (7) placed a rod upstream of a diffuser to increase the turbulence level in the flow. Although the turbulence level and velocity profile of the core of the flow entering the diffuser was not uniform, an increase in the peak pressure recovery of the diffuser of 21.5%, and a 38% increase in the pressure recovery at $2\theta = 20^{o}$ was observed. More recently, Sajben (8) eliminated separation and increased the pressure recovery of a conical diffuser as much as 16% by mounting a cylinder near the entrance to a diffuser.

Vortex generators, normally used in flows with adverse pressure gradients such as in diffusers and on airfoils, mix high energy air from outside the boundary layer, thereby delaying separation. The trailing vortex of the generators is the mixing mechanism. Vortex generator designs used to delay separation are described by Lachmann (9), Brown (10), Woolard (11), Taylor (12) and Gadetskiy(13). In one study, Senoo and Nishi (14) improved the performance of their conical diffuser by installing vortex generators three to eight times the inlet pipe diameter upstream of the diffuser entrance. Vortex generators arranged to create corotating vortices produced better results as compared to

vortex generators arranged to produce counterrotating vortices. The pressure recovery was increased approximately 15% when 2θ was 12°. They also noted that the vortex generators could prevent the flow in the conical diffuser from separating up to a total included angle of 16°. The pressure recovery with vortex generators never significantly exceeded the peak pressure recovery without generators.

Fiedler and Gessner (15) made an experimental investigation and an analytical study of the effectiveness of tangential fluid injection on the performance of two-dimensional diffusers. A significant improvement in the diffuser's performance by the tangential injection of fluid along the diverging walls was found at values of N/W_1 less than or equal to 4.0. For a large diverging angle (2θ larger than or equal to 20°), fluid injection located upstream of separation was found to be more effective, and the net effective performance (jet blowing power requirement included) was improved.

It is the purpose of this investigation to experimentally correlate turbulence parameters measured at the diffuser inlet with diffuser performance, and to thereby obtain an understanding of basic mechanisms which improve diffuser performance. This will lead to the design of systems where separation can be delayed for both internal and external flows when adverse pressure gradients exist, and consequently will be used to increase the pressure recovery, decreasing the drag, and/or increase heat transfer in systems utilizing fluid flow.

EXPERIMENTAL APPARATUS AND PROCEDURE

A. Experimental Apparatus

The experimental system used for the investigation, shown in Figure 1, consists of a baseplate and topplate for upstream rods, a throat, a straight channel, a test section, a plenum, a fan, and a noise attenuator. The fluid, air, is drawn through the system with a 5 horsepower centrifugal fan. The flow rate is controlled by adjusting a throttle which is located between the exit section of the fan and the inlet section of the noise attenuator. Screens and filters located in the plenum are used to improve flow conditions at the fan inlet. A hot wire anemometer system was used to obtain all velocity and turbulence measurements.

1. Throat and Straight Channel

The straight channel shown in Figure 2 was constructed out of clear lucite; the channel width dimension, W_1, is 1.024 in. (2.60 cm). The channel height/inlet width ratio (b/W_1) is 5.86 and the channel length/inlet width ratio (c/W_1) is 4.88. In the channel, boundary layers develop before entering the test section (diffuser). The channel has three sets of four pressure taps located upstream of the diffuser's inlet. The throat of the straight channel has an ASME standard nozzle shape. Masking tape applied to the throat served to reduce large fluctuations of boundary layer velocities at the diffuser inlet. It is believed that the masking tape caused transition from a laminar to a turbulent boundary layer to begin at the location of the tape rather than randomly along the channel walls.

2. Diffuser Section

The two-dimensional straight-walled diffuser used for this investigation was constructed out of clear lucite and is shown in Figure 2. The diffuser geometry is fixed by the aspect ratio, b/W_1, and any two of the four dimensionless geometric parameters: total included angle, 2θ, wall length ratio, L/W_1, center line length/inlet width ratio, N/W_1 and area ratio W_2/W_1. Throughout this experiment, the wall length ratio (L/W_1) remained fixed at a value of 14.7. The two diverging walls of the diffuser are positioned in the test section between a baseplate and a lid serving as a ceiling; weights were placed on top of the lid to insure a leak-free fit.

3. Turbulence Generation

Rods used for the turbulence generation were placed between the baseplate and topplate upstream of the throat as illustrated in Figure 3. The rod length/channel height ratio was fixed at 1.71 for all rod sets. Geometrical information about all upstream rod sets is presented in Table 1. The axes of the rods in rod set KH are parallel to the parallel walls of the diffuser, while the axes of all other rod sets are perpendicular to the parallel walls of the diffuser.

4. Instrumentation

The primary data recorded in this experiment were velocity profiles, turbulence levels, correlation coefficients, spectral density measurements and differential pressures across the diffuser. The velocity and turbulence measurements were obtained by using two Model 1010A Thermo-Systems Incorporated (T.S.I.) constant temperature hot wire anemometers, two Model 1005B linearizers, a Model 1015A correlator, and

. Hewlett-Packard (HP) Model 3400A true RMS meters. In order to obtain turbulence quantities averaged for ten second periods, the d.c. output from the rear panel of the RMS meter was fed into a HP Model 2212A voltage to frequency converter, and then into a HP Model 5223L electronic counter. A Hewlett-Packard Model 3581A wave analyzer was used to obtain longitudinal spectral density measurements. Time delays and an electronic multiplier were constructed and used in the determination of longitudinal autocorrelation coefficients. A capacitor-induction type delay line was fabricated for use with time delays of less than 30 μ sec.. Reticon type TAD-32A and type SAD-1024A analog delay lines were used in the fabrication of time delay lines of 32 μ sec. and larger. A Motorola type MC 1594L multiplier and a type MC 1556G integrator were used in the fabrication of the electronic multiplier. In order to obtain the wire's sensitivity to velocity components parallel to the wire, all inclined hot wires were calibrated using a T.S.I. Model 1125 calibrator, a Meriam Model 34FB2 TM micromanometer, and a Doric Model DS-100 digital voltmeter.

B. Procedure

The techniques used to obtain the data presented in this report are presented below. All data were taken with an inlet Reynolds number, based on the mass average velocity and width of the channel, of 7.83×10^4. All hot wire anemometer measurements were obtained with the diffuser walls removed and with the probe body aligned parallel to the flow.

1. Boundary Layer Parameters

In order to determine the boundary layer characteristics at the diffuser inlet (Section 1), velocity profiles were obtained at the channel exit using a single hot wire mounted in a micrometer travers-

ing device. From the data obtained, dimensionless plots of $\bar{u}/U_m$ and $(\bar{u}/U_m)^2$ versus the dimensionless distance y/W_1 were constructed. Based on these plots, values of boundary layer displacement thickness (δ^*), momentum thickness (δ^{**}), and shape factor (H) were obtained.

2. Turbulence Measurements

When the velocity readings were recorded, RMS values were simultaneously recorded. These data were again normalized by the free-stream velocity, and became the turbulence levels ($\sqrt{u'^2}/U_m$) which were also plotted as a function of y/W_1.

Free-stream turbulence levels in the y and z directions were obtained using both an X-configuration probe, and from the results of single wires placed perpendicular and inclined 45^o to the mean flow direction. The relatively large size of the X-wire configuration and inclined 45^o probes compared to that of the boundary layer prohibited the use of them within the boundary layer. Equations presented by Durst (16) were used to calculate the turbulence intensities.

Free-stream longitudinal correlation coefficients and spectral density measurements were obtained using a single wire placed normal to the flow. Values of the longitudinal integral scale of turbulence (λ_x) were obtained by integration of the area under curves of the longitudinal correlation coefficient versus a distance corresponding to the time delay of the hot wire signal (Taylor's hypothesis (17)).

All presented turbulence measurements were obtained using 0.00015 in. (0.004mm) dia. tungsten wires with a 0.02 in. (0.5mm) sensing length and a sensing length/total length between the supports ratio of 0.33. T.S.I.

Model 1210 straight probes, Model 1213 45° probes, and Model 1241 "X" probes for end flow, modified with a 0.005 in. (0.13mm) spacing between the wires, were used.

As recommended by Rasmussen (18), the 100,000 Hz low pass filter of the anemometer was used for all hot wire measurements to eliminate high frequency components of the anemometer self noise. The frequency at which the closed loop response of the hot wire anemometer system was attenuated 3db, obtained by the method of Freymuth (19), was in excess of 40,000 Hz for all hot wires used.

3. Diffuser Pressure Rise Measurements

Pressure taps are located $0.25W_1$ upstream from the end of each diffuser wall. The pressure rise across the diffuser was determined by taking the difference between this pressure and the value of the pressure at the exit of the channel (Section 1), obtained by extrapolating the static pressures measured in the channel. This extrapolation utilized the power law relationship for boundary layer growth ($\delta^* \simeq x^{0.8}$) (20). A pressure differential between the pressure from taps located in the topplate and baseplate upstream of the rods and the extrapolated pressure at Section 1 was used to determine the free-stream channel velocity and corresponding value of inlet mass average velocity. The correction associated with the extrapolation of the channel static pressures increased the diffuser's static pressure recovery coefficient by a maximum of 1.4 percent. A pressure loss coefficient across the rods (C_f), normalized by the kenetic energy at Section 1, was calculated for each rod set using the pressure loss across a screen as a function of solidity ratio presented by Hoerner (21). The maximum pressure loss coefficient of any rod set was less

than one percent and was ignored in diffuser static pressure coefficient calculations. Inclined manometers were used for all pressure measurements.

RESULTS AND DISCUSSION

A description of the flow characteristics at the diffuser inlet for the upstream rod sets, results from the pressure recovery measurements of the diffuser and correlations between the static pressure recovery coefficients of the diffuser and inlet free-stream turbulence parameters are described below. A pictorial representation of the flow characteristics at the diffuser inlet is presented in Figure 4.

A. Inlet Velocity and Longitudinal Turbulence Profiles

Typical velocity profiles at the diffuser inlet are presented in Figure 5. The average dimensionless inlet blockage parameter, $2\delta^*/W_1$, obtained from the velocity profiles for all rod configurations was 0.040. The uncertainty in this quantity, obtained using the method of Kline and McClintock (22) with 20:1 odds, was ± 5% for the no rod case and rod sets A through D, and was ± 10% for rod sets E through L. The percent difference from the average value of $2\delta^*/W_1$ was less than the percent uncertainty for each rod set. Kline (23) also found small changes in the velocity profile of a turbulent boundary layer when free-stream longitudinal turbulence intensities were varied to 4% (all presented results have longitudinal turbulence intensities less than 3.07%). The rod set geometries produced velocity profiles with an average shape factor of 1.56, a value expected for a turbulent boundary layer in the final stage of transition. A shape factor of 1.4 would be expected for a fully developed turbulent boundary layer, and a shape factor of 2.6 to 2.7 would be expected for a laminar boundary layer (20). A velocity profile obtained using the law of the wall and the velocity defect equation (24) with the same experimentally determined displacement thickness is also presented in Figure 5. Velo-

city profiles obtained at several positions ($z/b = \pm 0.33$) produced essentially the same results.

Longitudinal turbulence level traverses within the boundary layer for the no rod case, and rod sets D, H, and K are presented in Figure 6. The results indicate that the free-stream turbulence significantly alters the turbulent structure of the boundary layer. Ahmad (25) found that both the free-stream turbulence level and the free-stream longitudinal scale of turbulence significantly alter the turbulence level and the scale of turbulence within the boundary layer. Turbulence level traverses for turbulent boundary layers with low free-stream turbulence levels obtained by Klebanoff (26) and Schubauer (27) are also presented in Figure 6; a reasonably good agreement with the presented results for the case of no upstream rods is obtained.

All velocity profiles show a uniform core velocity in the center 75 percent of the channel. The region in which turbulence levels were uniform varied from the center 30 percent of the channel for rod sets with $D/W_1 = 4.39$, to the center 70 percent of the channel for the no rod condition.

B. Free Stream-Turbulence Parameters

Values of the turbulence intensity in the flow direction ($\sqrt{\overline{u'^2}}/U_m$) and in the y direction ($\sqrt{\overline{v'^2}}/U_m$) for all of the rod sets are presented in Table 1. The uncertainties in the measurements are approximately 5 percent for rod sets A through H and approximately 10 percent for the no rod case and rod sets I through L. The free-stream turbulence intensities obtained using the single wire method agree well with those obtained using the X-wire. The ratio of the free-stream RMS turbulence intensity in the z direction to the RMS turbulence intensity in the y direction was 0.88 for all rod sets except for rod set KH, and was 0.75 for rod set KH. The value of the wire's sensitivity coefficient to velocity components parallel to the wire (16) varied from 0.16 to 0.20 for the inclined wires used.

Spectral density curves for the longitudinal component of turbulence are presented in Figures 7a through 7e. The curves show a broadband turbulence without peaks of power at any one frequency. The curves for the larger diameter rods show a larger percentage of low frequency power as compared to the curves for the smaller diameter upstream rods.

The integral scale of turbulence values, λ_x, were obtained by integration under the correlation coefficient curves, examples of which are presented in Figure 8. Values of the integral scale of turbulence in the flow direction, transformed dimensionless by dividing by the average inlet boundary layer displacement thickness, are also presented in Table 1. The uncertainty in this quantity varies from approximately 10 percent for rod sets A through D to approximately 15 percent for rod sets E through L.

C. Diffuser Performance

Results of the diffuser's static pressure recovery coefficient as a function of diffuser area ratio and total included divergence angle for Reneau's results (28) at values of $2\delta^*/W_1$ of 0.030 and 0.050 are compared to the results of this study ($2\delta^*/W_1 = 0.040$) for the case of no upstream rods in Figure 9. Good agreement is achieved for total included divergence angles less than 4°, although the results of Reneau at a value of $2\delta^*/W_1 = 0.040$ (an average of Reneau's results at values of $2\delta^*/W_1 = 0.030$ and 0.050) are as much as 10 percent lower compared to those of this study in the region of the peak pressure recovery coefficient. The agreement seems reasonable considering that the results presented by Reneau are correlations of measurements from a wide variety of data and that geometrical differences (e.g., the length of the flexible section of the diffuser's throat) may exist between various test systems.

Data for the static pressure recovery coefficient at total divergence angles of 12° and 20° for all of the rod sets are presented in Table 1. The uncertainty in these coefficients is approximately 5 percent. Static pressure recovery coefficients are presented as a function of diffuser area ratio in Figures 10a through 10e. The results indicate that increases in the static pressure recovery coefficient of 22.8% at $2\theta = 20^{\circ}$, and 11.4% at $2\theta = 12^{\circ}$ are obtained for the K rod set as compared to the no-rod case. The percentage increase of C_p at $2\theta = 20^{\circ}$ is more than four times the uncertainty. The peak pressure recovery coefficient was increased 9.7% and the total included divergence angle corresponding to the peak recovery coefficient increased approximately 1.5 degrees. Since all rod geometries produce essentially the same velocity profile at the diffuser's inlet, the increase in diffuser performance can be attributed to differences in turbulence quantities at the diffuser's inlet.

Values of C_p at $2\theta = 12^{\circ}$ and 20° are presented as a function of $\sqrt{\overline{u'^2}}/U_m$ in Figure 11. The values of C_p are relatively insensitive to $\sqrt{\overline{u'^2}}/U_m$; for example, the values of C_p vary significantly ($0.570 \leq C_p$ ($2\theta = 20^{\circ}$) ≤ 0.700) for values of $1.75 \leq \sqrt{\overline{u'^2}}/U_m \leq 2.14$.

Values of C_p at $2\theta = 20^{\circ}$ are presented as a function of $\sqrt{\overline{v'^2}}/U_m$ in Figure 12 and as a function of $\sqrt{\overline{q'^2}}/U_m$ in Figure 13. The results show a general trend of obtaining larger values of C_p with larger values of $\sqrt{\overline{v'^2}}/U_m$ and $\sqrt{\overline{q'^2}}/U_m$, but the trend is not consistent (e.g., rod set E produces relatively high turbulence intensities, but the corresponding values of C_p are lower compared to those obtained with some rod sets producing lower turbulence intensities. The results show that a threshold turbulence intensity in the y direction of about 3 percent or a total turbulence intensity of about 2.5 per-

cent is required to obtain increases in diffuser performance as compared to the no-rod case. All of the largest values of C_p (C_p ($2\theta = 12^o$) $\geq$ 0.78 and C_p ($2\theta = 20^o \geq 0.69$) were obtained with values of $\sqrt{v'^2}/U_m$ and $\sqrt{q'^2}/U_m$ equal to or larger than 4.46 and 3.73 percent respectively. It appears that the turbulence intensity in the y direction and the total turbulence intensity are important parameters, but are not the only parameters affecting diffuser performance.

In Figure 14, values of C_p at $2\theta = 12^o$ and 20^o are presented as a function of λ_x/δ^*. The values of C_p show a general trend of obtaining larger values of C_p with larger values of λ_x/δ^*, but again the trend is not consistent. All of the largest values of C_p (C_p ($2\theta = 12^o$) $\geq$ 0.78 and C_p ($2\theta = 20^o$) $\geq$ 0.68) were obtained with values of $\lambda_x/\delta^* \geq 7.53$ (or with minimum values of λ_x about 25% larger than the boundary layer thickness).

To investigate the existence of a possible correlation between the pressure recovery coefficient, the scale of turbulence at the diffuser inlet, and the total RMS turbulence intensity, a graph of these parameters was constructed as shown in Figure 15. Values of C_p ($2\theta = 20^o$) are listed next to each data point along with, in parentheses, values of C_p ($2\theta = 12^o$). A correlation of the data does exist, which shows that larger values of both the total turbulence intensity and the scale of turbulence in the flow direction result in larger values of the pressure recovery coefficient. The results suggest that a larger scale of turbulence more effectively transmits the free-stream turbulence generated by the rods to the diffuser walls. This larger scale of turbulence coupled with larger values of the total RMS turbulence intensity could result in a decrease of the distortion within the diffuser and a delay of separation, which could correspondingly produce

larger values of the pressure recovery coefficient. A study of the effect of free-stream turbulence on a boundary layer by Arnel (29) using free-stream total turbulence intensities of about 5 percent showed a decrease in the shape factor of the boundary layer which would correspondingly delay separation. The curves in Figure 15 show that in order to obtain increases of C_p ($2\theta = 20^o$) of 21.1% and increases of C_p ($2\theta = 12^o$) of 11.4%, minimum values of λ_x/δ^* and $\sqrt{\overline{q'^2}}/U_m$ must be 7.5 and 3.5 percent respectively.

The results of this preliminary study suggest that the free-stream scale of turbulence and turbulence intensity are important parameters, but these may not be the only parameters affecting diffuser performance (or the delay of separation for the case of external flows). In this limited study, values of the integral scale of turbulence in the y and z directions were not measured; also $\sqrt{\overline{v'^2}}$ / $\sqrt{\overline{w'^2}}$ was a constant for almost all rod sets, and $\sqrt{\overline{v'^2}}$ / $\sqrt{\overline{u'^2}} \geq 1.73$ for all rod sets. It was observed that the free-stream turbulence altered the turbulence structure of the boundary layer; perhaps other means of altering the turbulence structure of the boundary layer would result in similar improvements in diffuser performance.

CONCLUSIONS

An experimental investigation of the influence of free-stream turbulence on the performance of a subsonic two-dimensional diffuser has been made. The diffuser wall length/inlet width ratio was 14.7 and the inlet blockage parameter, $2\delta^*/W_1$, was 0.040. The diffuser's pressure recovery coefficient at a total included divergence angle of 20^o was increased 21.1 percent, the peak pressure recovery coefficient was increased 9.7 percent, and the total included divergence angle corresponding to the peak pressure recovery coefficient was increased approximately 1.5 degrees when values of the inlet free-stream integral scale of turbulence in the flow direction were greater than 7.5 times the inlet boundary layer displacement thickness, and when the inlet total turbulence intensity was greater than 3.5 percent. The free-stream turbulence was found to significantly affect the turbulence intensities within the boundary layer, but did not significantly alter the velocity profile of the boundary layer at the diffuser's inlet. The results of the study suggest basic mechanisms that can be used to delay separation. They may be applicable for both internal and external flows for improvement of heat transfer and/or lift, drag or pressure recovery coefficients when the turbulence is generated with low losses (e.g., near stagnation regions).

FUTURE INVESTIGATIONS

In this preliminary study, a correlation between free-stream turbulence parameters and improved diffuser performance has been found. Some future possible studies are listed below.

1. Measurement of the integral scale of turbulence in the y and z directions will indicate if correlations between these parameters, or eddy volume, and diffuser performance exist.
2. Measurement of the turbulence parameters within the boundary layer and free-stream turbulence-boundary layer interactions within the diffuser may aid the understanding of the basic mechanisms which cause the increases in diffuser performance. If the turbulence conditions within the boundary layer which correlate with high diffuser performance are known, then these conditions may be able to be obtained without free-stream turbulence. This study would show if free-stream turbulence is necessary for improved diffuser performance, or is only a mechanism used to alter the boundary layer characteristics within the diffuser.
3. Observe the influence of free-stream turbulence on diffuser performance using different values of $2\delta^*/W_1$, L/W_1, and $\sqrt{\overline{v'^2}}$ / $\sqrt{\overline{w'^2}}$ as compared to those used in this study.
4. Study the effect of free-stream turbulence with external flows. The generation of turbulence using serrations near stagnation regions of airfoils or automobiles, or by other methods, may lead to improved lift and drag coefficients.

5. Mathematical modeling of free-stream turbulence-boundary layer interactions may lead to the detection of important governing parameters, and to the extent of possible improvements with these parameters.

   Flow visualization studies will help to understand the basic mechanisms involved in improving diffuser performance.

7. Additional studies using upstream rods with their axes positioned parallel to the parallel walls of the diffuser may indicate if the orientation of the axes of the rods and corresponding axes of the vortices is an important parameter affecting diffuser performance. If two rod sets with different rod axis orientations produce the same free-stream turbulence intensities and scales of turbulence but different pressure recovery coefficients, then one could attribute the difference in diffuser performance to the orientation of the axes of the vortices.

ACKNOWLEDGEMENTS

This project was sponsored by NASA-ARC Grant #NSG-2391. The author gratefully acknowledges the work of graduate students Masao Fukuda, Yu Hang Ho, and James Ross, and of student assistants Michael Dudley, John McCrillis, Michael Reinath, and Philip Snyder.

REFERENCES

1. Cockrell, D. J. and Markland, E., "A Review of Incompressible Diffuser Flow", Aircraft Engineering 35, pg. 286-92, Oct. 1963.

2. McDonald, A.T. and Fox, R.W., "An Experimental Investigation of Incompressible Flow in Conical Diffusers", ASME Paper No. 65-FE-25, 1965.

3. Sovran, G. and Klomp, E.D., "Experimentally Determined Optimum Geormetries for Rectilinear Diffusers with Rectangular, Conical or Annular Cross-Section", from Fluid Mechanics of Internal Flow, edited by G. Sovran, Elsevier Publishing Co., Amsterdam, pg. 270-319, 1967.

4. Moore, C.A. Jr. and Kline, S.J., "Some Effects of Vanes and of Turbulence on Two-Dimensional Wide Angle Subsonic Diffusers", Department of Mechanical Engineering, Stanford University, Sept. 1, 1955.

5. Fox, R.W. and Kline, S.J., "Flow Regime Data and Design Methods for Curved Subsonic Diffusers", TASME, Journal of Basic Engineering, Series D., Vol. 84, pg. 303-312, 1962.

6. Smith, C.R. Jr., and Kline, S.J., "An Experimental Investigation of the Transitory Stall Regime in Two-Dimensional Diffusers Including the Effects of Periodically Disturbed Inlet Conditions", Department of Mechanical Engineering, Stanford University, Aug. 1971.

7. Waitman, B.A., Reneau, L.B., and Kline, S.J., "Effects of Inlet Conditions on Performance of Two-Dimensional Diffusers", Journal of Basic Engineering, Trans. ASME, Series D., Vol. 83, pg. 349-360, 1961.

8. Sajben, M., Chen, C.P. and Kroutel, J.C., "A New Passive Boundary Layer Control Device", Journal of Aircraft, Vol. 14, No. 7, pg. 654-660, July 1977.

9. Lachmann, G.V., "Boundary Layer and Flow Control", Vol. 2, Pergamon Press, New York, 1961.

10. Brown, A.C., Nawrochi, H.F., and Palez, P.N., "Subsonic Diffusers Designed Integrally with Vortex Generators", Journal of Aircraft, Vol. 5, No. 3, pg. 221-229, May/June 1968.

11. Woodard, H.W., Benson, J.L. Stroud, J.F., Drell, H., "Boundary Layer Forced Mixing Investigation - Literature Survey and Progress Report", Lockheed California Co., Report LR 18478, Nov. 1965.

12. Taylor, H.D., "Application of Vortex Generator Mixing Principles to Diffusers". Concluding Report, United Aircraft Corp., Research Dept., Report R-15064-5, Dec. 31, 1948.

13. Gadetskiy, V.M., Serebrizskig, Ya. M., and Fomin, V.M. "Investigation of the Influence of Vortex Generators on Turbulent Boundary Type Separation," NASA Technical Trans., NASA TT-F-16, 056, 1972.

14. Senoo, Y., and Nishi, M., "Improvement of the Performance of Conical Diffuser by Vortex Generators", Journal of Fluids Engineering, pg. 4-10, March 1974.

15. Fiedler, R.A., and Gessner, F.B., "Influence of Tagential Fluid Injection on the Performance of Two-Dimensional Diffusers", ASME Paper No. 72-FE-16, 1972.

16. Durst, F., "Hot Wire and Laser-Doppler Techniques in Turbulence Research", Report SFB 80/EM/119, Universitat Karlsnuke, Germany, Dec., 1977.

17. Hinze, J.O., Turbulence, 2nd edition, McGraw-Hill Book Co., N.Y., 1975.

18. Rasmussen, C.G., "Measurement of Turbulence Characteristics", DISA Information No. 3, Jan., 1966.

19. Freymuth, Peter, "Feedback Control Theory for Constant Temperature Hot Wire Anemometers", The Review of Scientific Instruments, Vol., 38, No. 5 May 1967, pg. 677-681.

20. Schlichting, Hermann, Boundary Layer Theory, 6th ed., McGraw-Hill Book Co., N.Y., 1968.

21. Hoerner, Sighard F., "Fluid Dynamic Drag", Published by the author, pg. 323, 1958.

22. Kline, S. J. and McClintock, F.A., "Describing Uncertainties in Single Sample Experiments", Mechanical Engineering, pg. 3-8, Jan., 1953.

23. Kline, J. J., Lisin, A.V., and Waitman, B.A., "Preliminary Experimental Investigation of Effects of Free Stream Turbulence on Turbulent Boundary Layer Growth", NASA TN D-368, March, 1960.

24. Daily, J. W. and Harleman, D. R., Fluid Dynamics, Addition-Wesley Publishing Co., Inc., 196[illegible]

25. Ahmad, Q.A., Luxton, R.E., and Antonia, R.A., "Characteristics of a Turbulent Boundary Layer with an External Turbulent Uniform Shear Flow", J. Fluid Mech., Vol. 37, Part 2, pg. 369-396, 1976.

26. Klebanoff, P.S., "Characteristics of Turbulence in a Boundary Layer with Zero Pressure Gradient", NACA Rep. No. 1247, 1955.

27. Schubauer, G.B., "Turbulent Processes as Observed in Boundary Layer and Pipe Flow", Journal of Applied Physics, Vol. 25, No. 2, Feb., 1954.

28. Reneau, L.R., Johnston, J.P., and Kline, S.J., "Performance and Design of Straight, Two-Dimensional Diffusers", ASME Paper No. 66-FE-10, Apr., 1966.

29. Arnal, D., Cousteix, J. and Michel, R., "Couche Limite se Developpant Avec Gradient de Pression Positif Dans un Ecoulement Exterieur Turbulent", Resh. Aerospatiale (Janvier-Fevrie) pg. 13-26, 1976

TABLE 1 SUMMARY OF RESULTS

Rod Set	D/W_1	r/W_1	n	$C_p(2\theta = 12^o)$	$C_p(2\theta = 20^o)$	$\sqrt{\overline{u'^2}}/U_m(\%)$	$\sqrt{\overline{v'^2}}/U_m(\%)$	λ_x/δ^*
None	-	-	0	0.700	0.570	0.88	2.03	-
A	0.18	2.93	19	0.700	0.570	1.75	3.02	4.28
B	0.18	4.39	35	0.700	0.585	1.31	2.89	6.10
C	0.37	2.93	11	0.731	0.639	2.03	4.05	4.35
D	0.37	3.90	11	0.720	0.615	1.58	3.60	6.95
E	1.28	2.93	3	0.745	0.655	3.07	5.49	6.38
F	1.28	4.39	5	0.785	0.690	2.10	4.46	7.53
G	1.28	5.85	7	0.770	0.675	1.28	3.83	8.37
H	1.28	5.51	7	0.765	0.670	1.53	3.89	7.92
I	4.39	8.78	3	0.745	0.605	1.05	4.04	10.55
J	4.39	7.80	3	0.772	0.675	1.57	5.14	11.61
K	4.39	9.76	5	0.780	0.700	2.05	6.32	9.17
KH	4.39	9.76	5	0.753	0.680	2.99	8.91	8.72
L	4.39	6.83	3	0.780	0.690	2.14	5.87	10.27

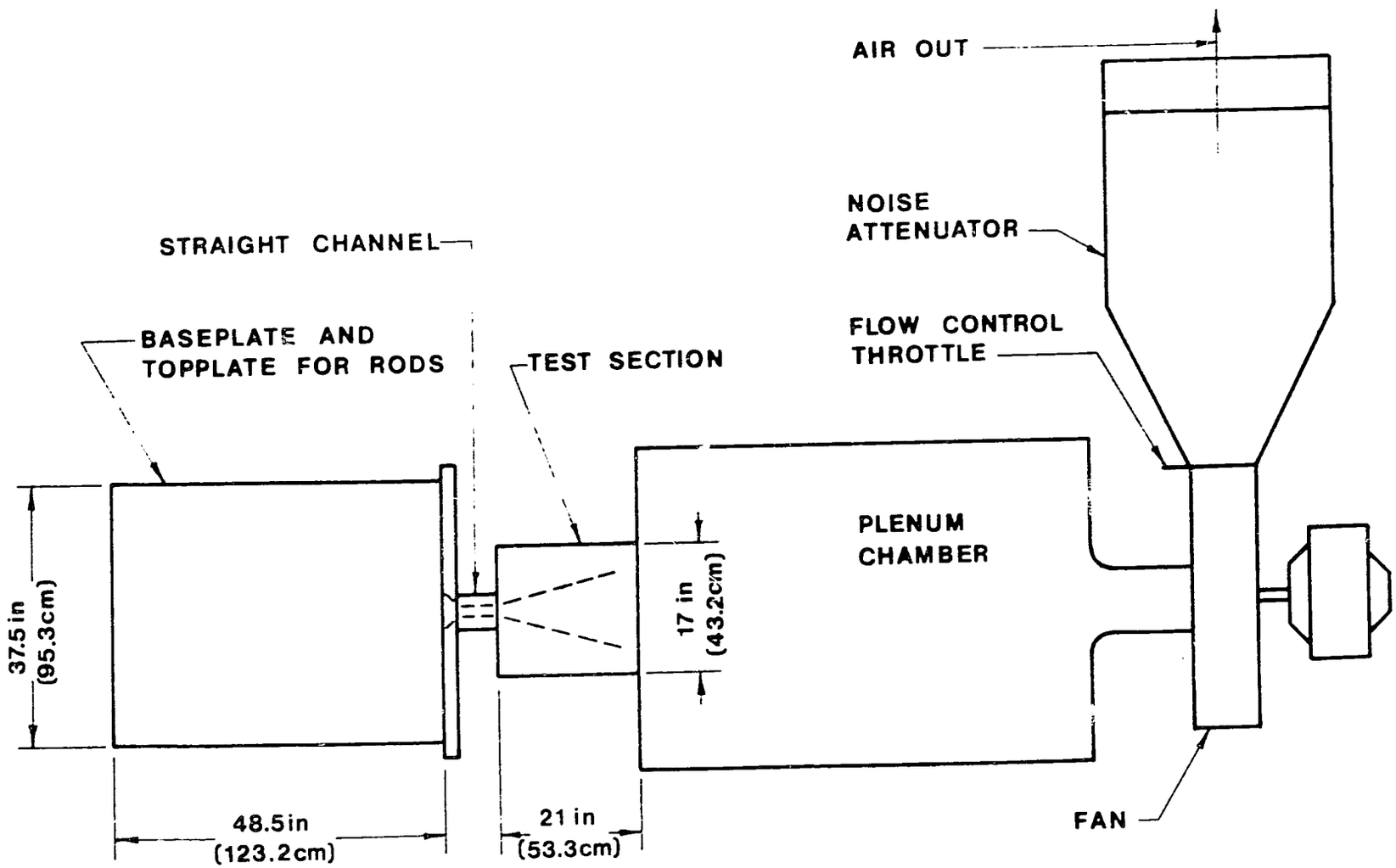

(TOP VIEW)

Figure 1

Experimental System

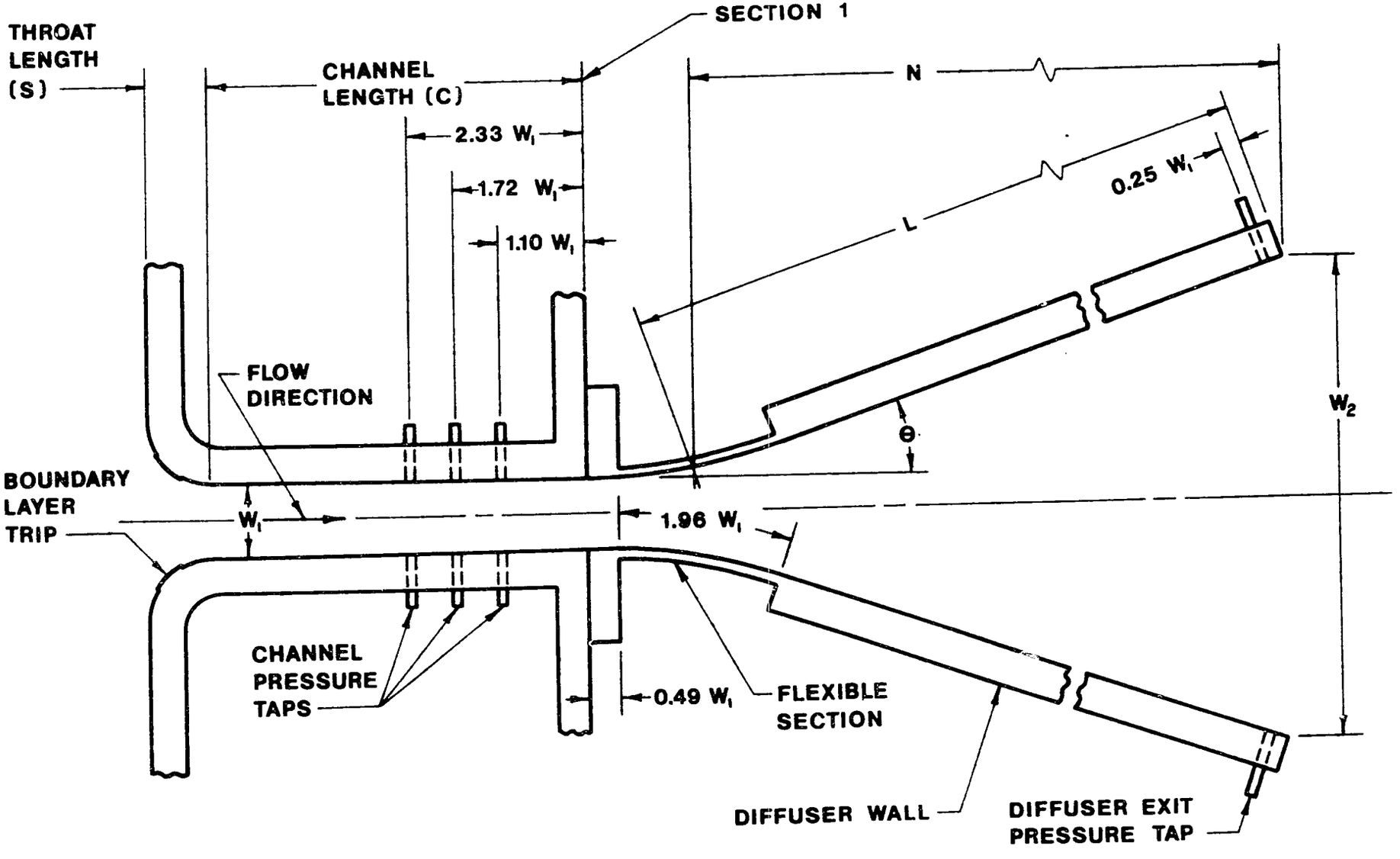

Figure 2

Inlet, Channel and Diffuser

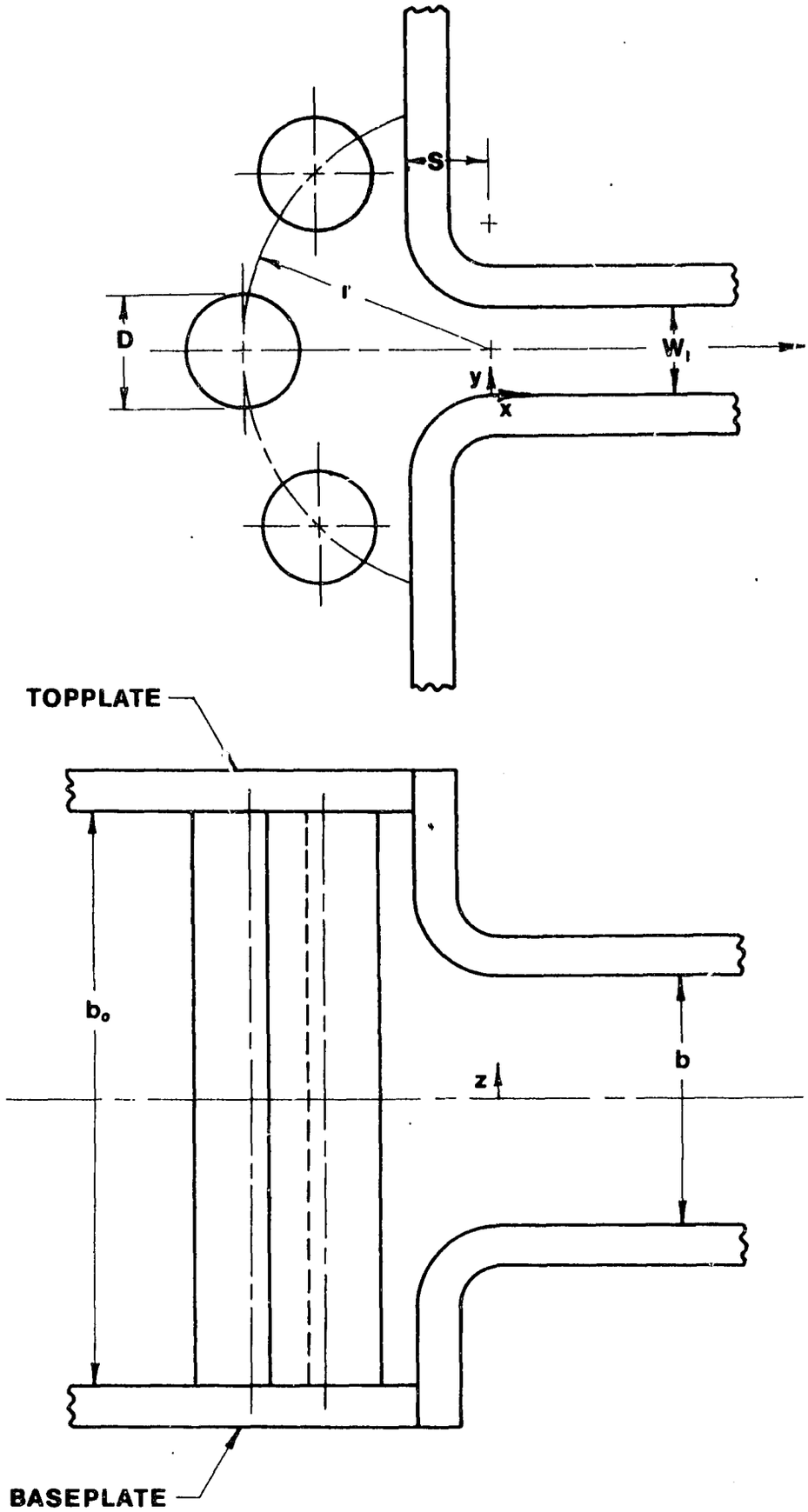

Figure 3

Rod Set Geometry Nomenclature

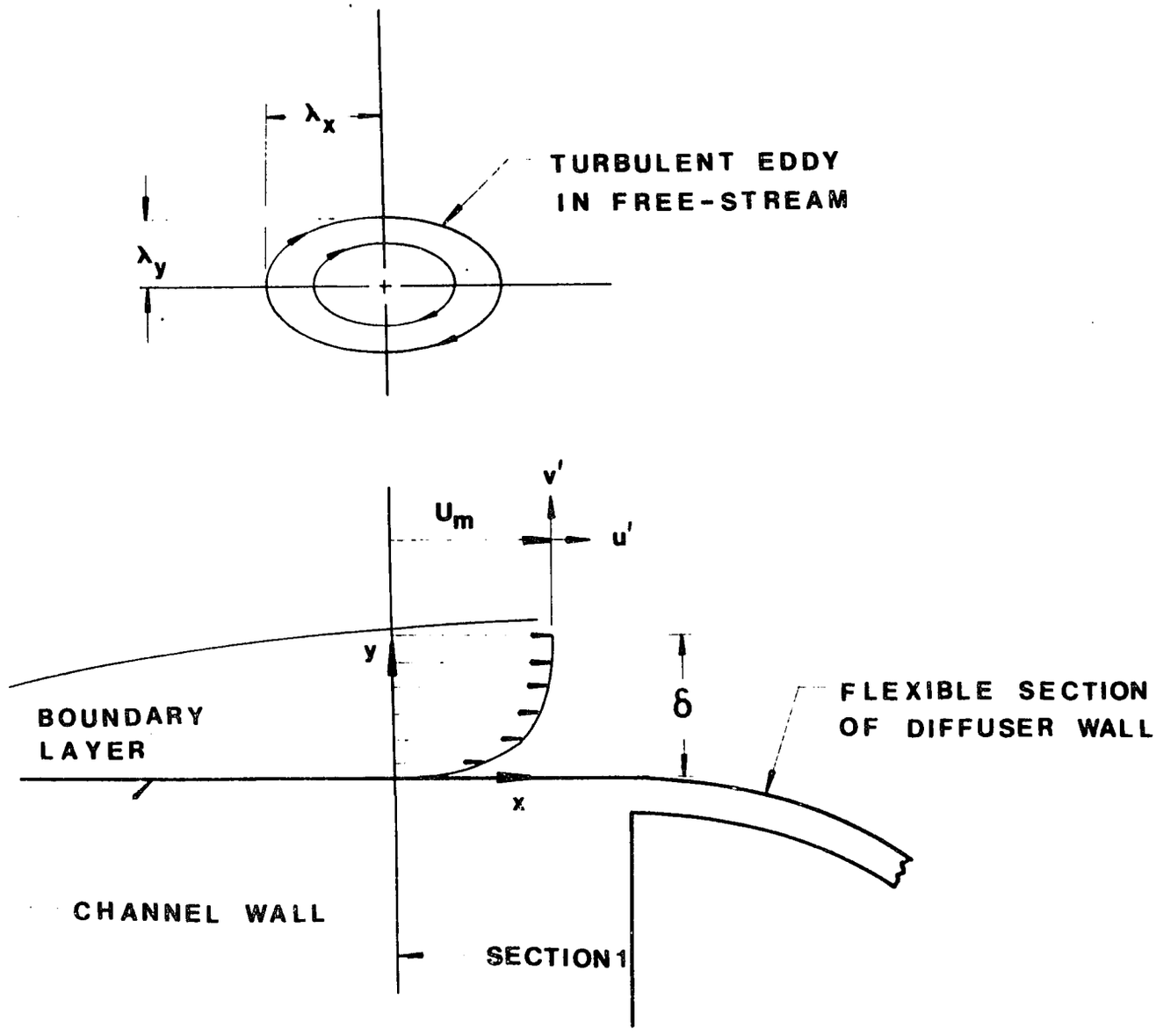

Figure 4

Two-Dimensional Schematic of Flow
Characteristics at Diffuser Inlet

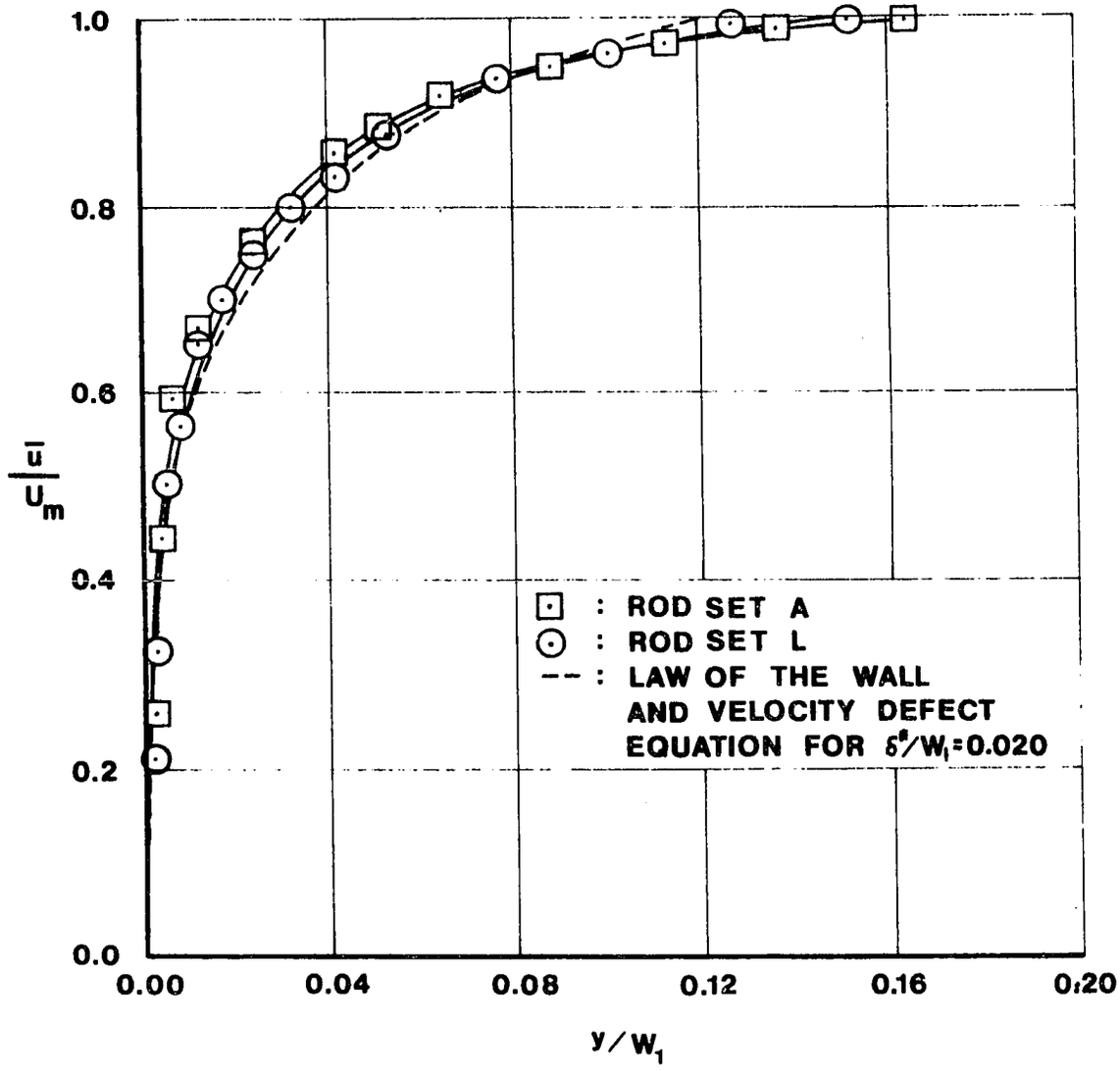

Figure 5

Inlet Boundary Layer Velocity Profiles

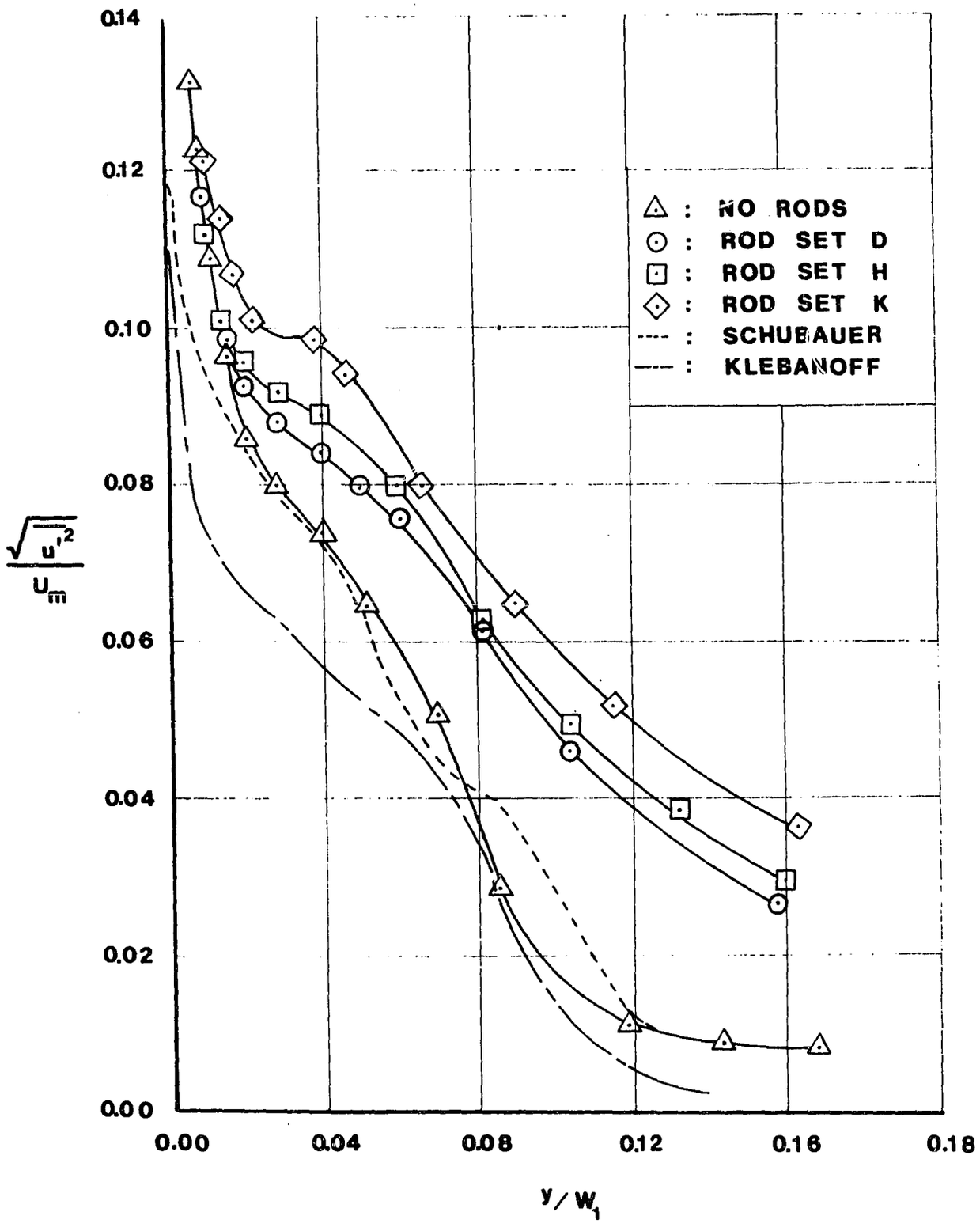

Figure 6

Inlet Boundary Layer Longitudinal Turbulence Profiles

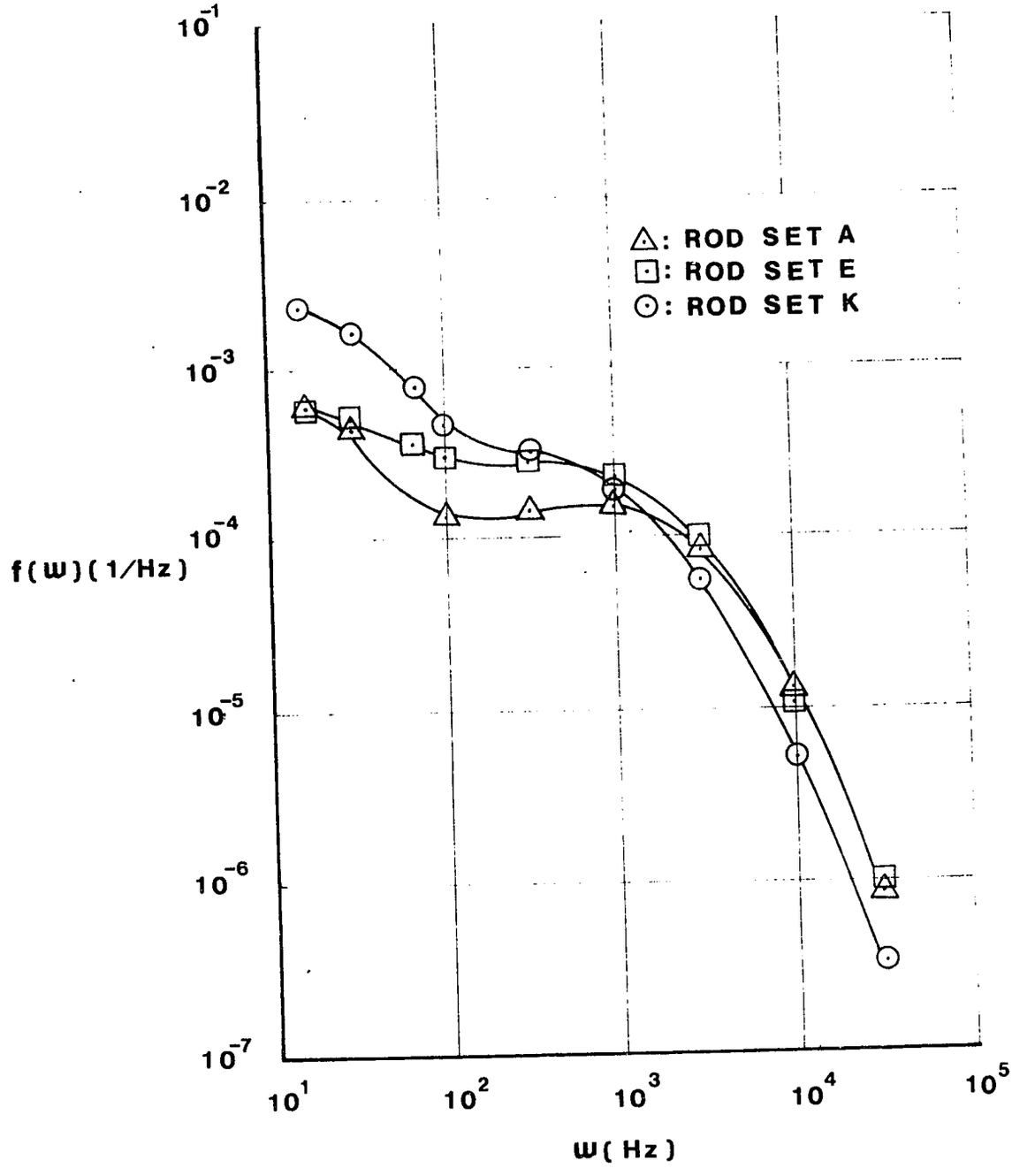

Figure 7a

Spectral Density Curves of Inlet Free-Stream Turbulence

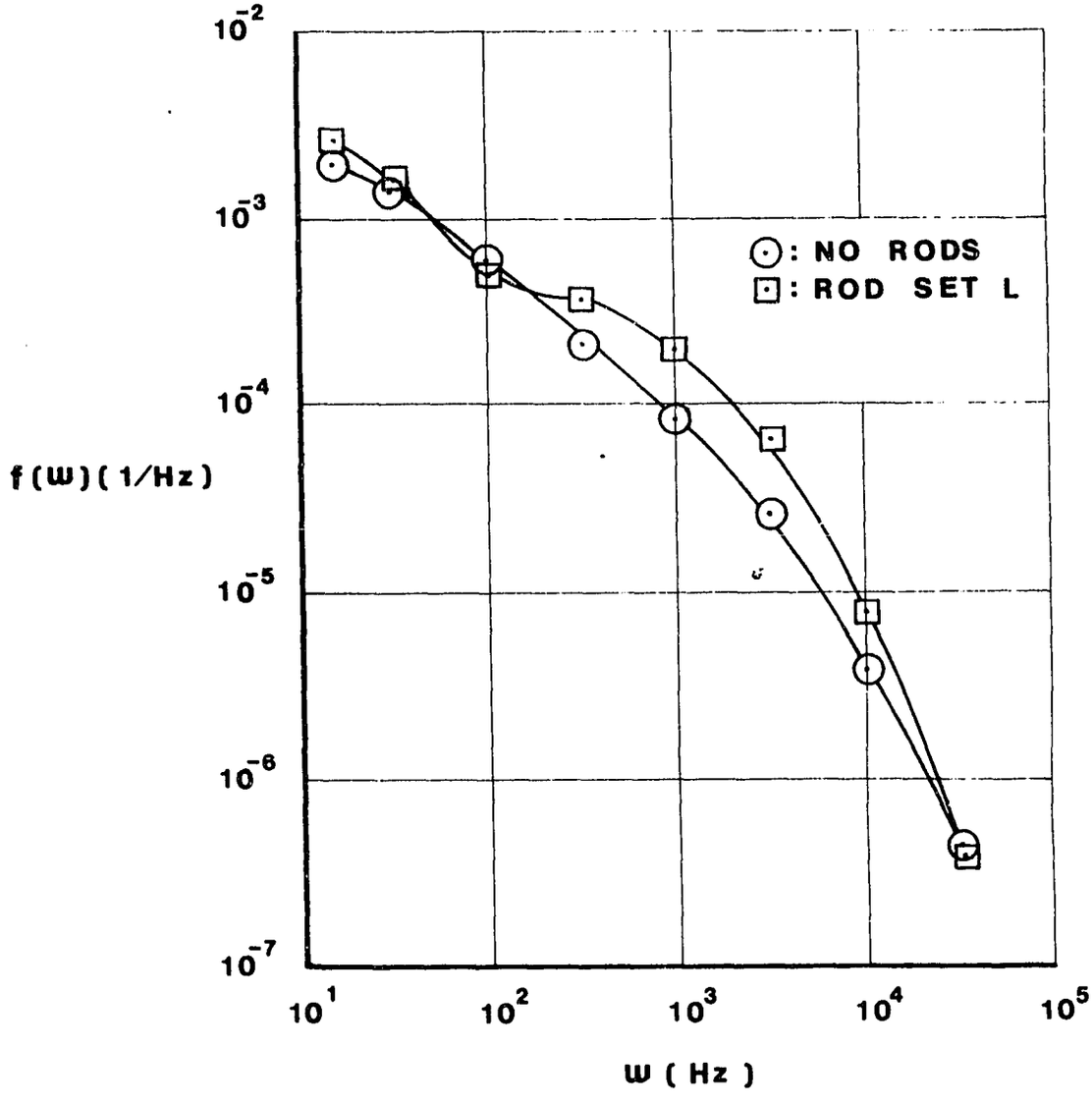

Figure 7b

Spectral Density Curves of Inlet Free-Stream Turbulence

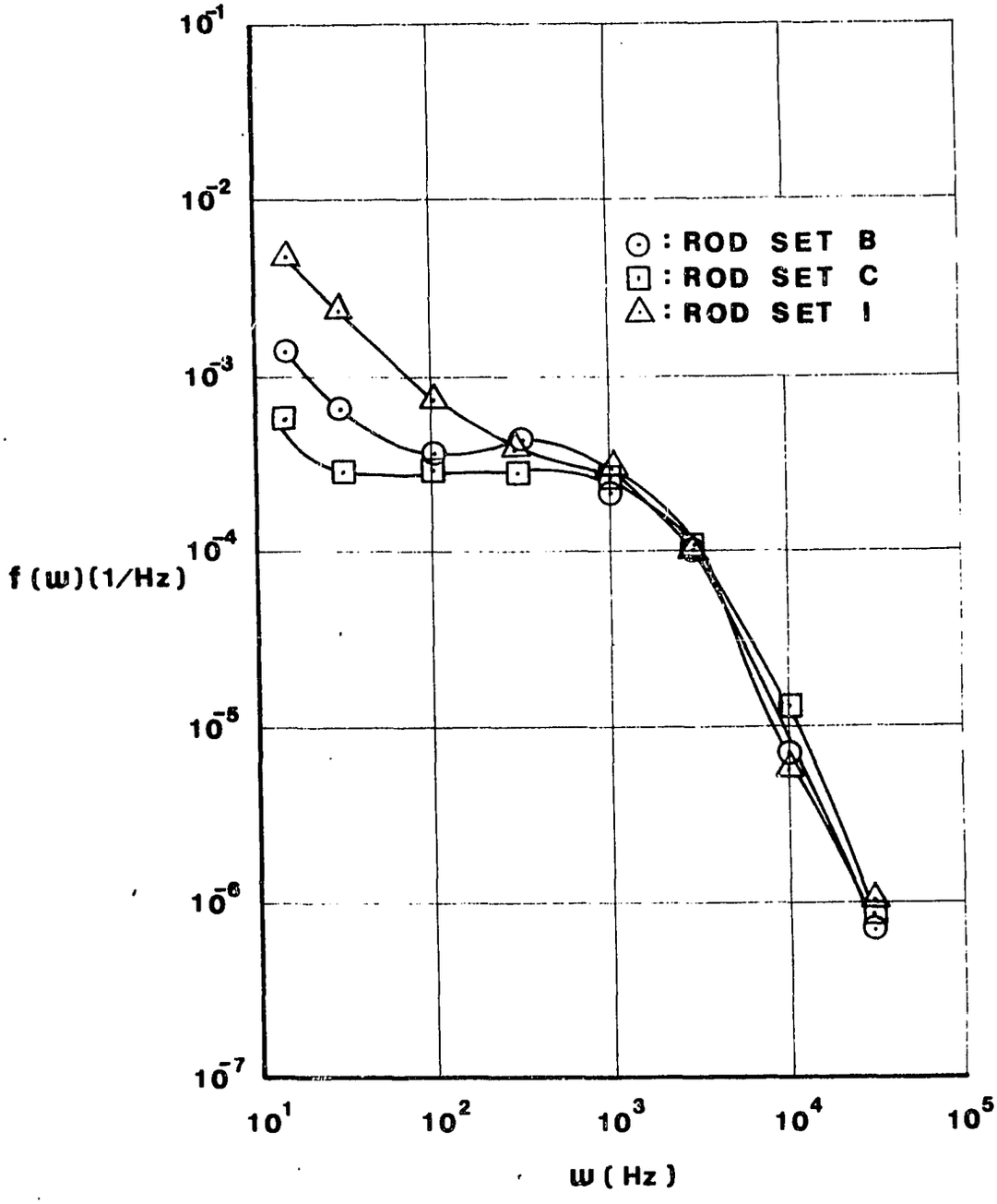

Figure 7c

Spectral Density Curves of Inlet Free-Stream Turbulence

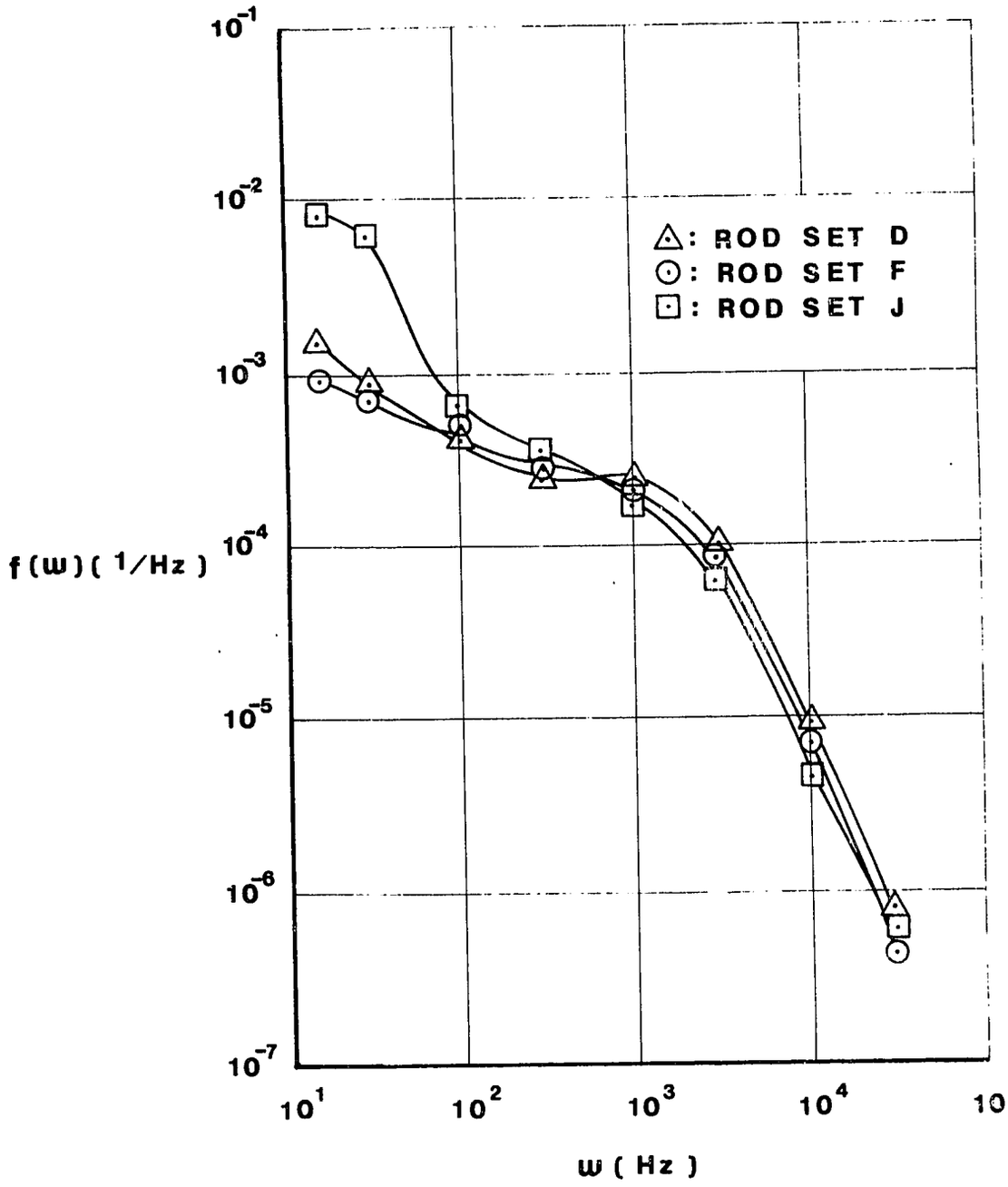

Figure 7d

Spectral Density Curves of Inlet Free-Stream Turbulence

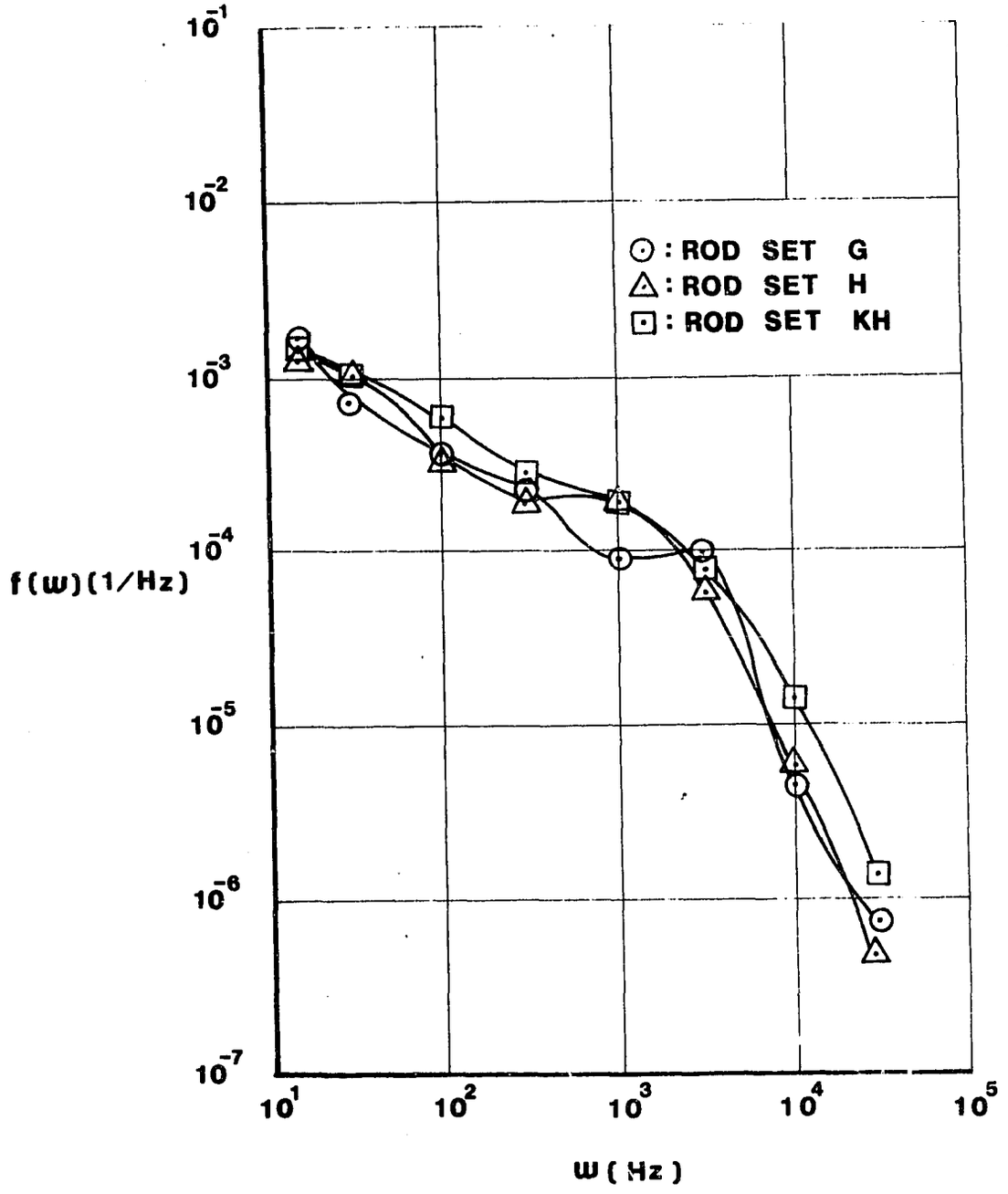

Figure 7e

Spectral Density Curves of Inlet Free-Stream Turbulence

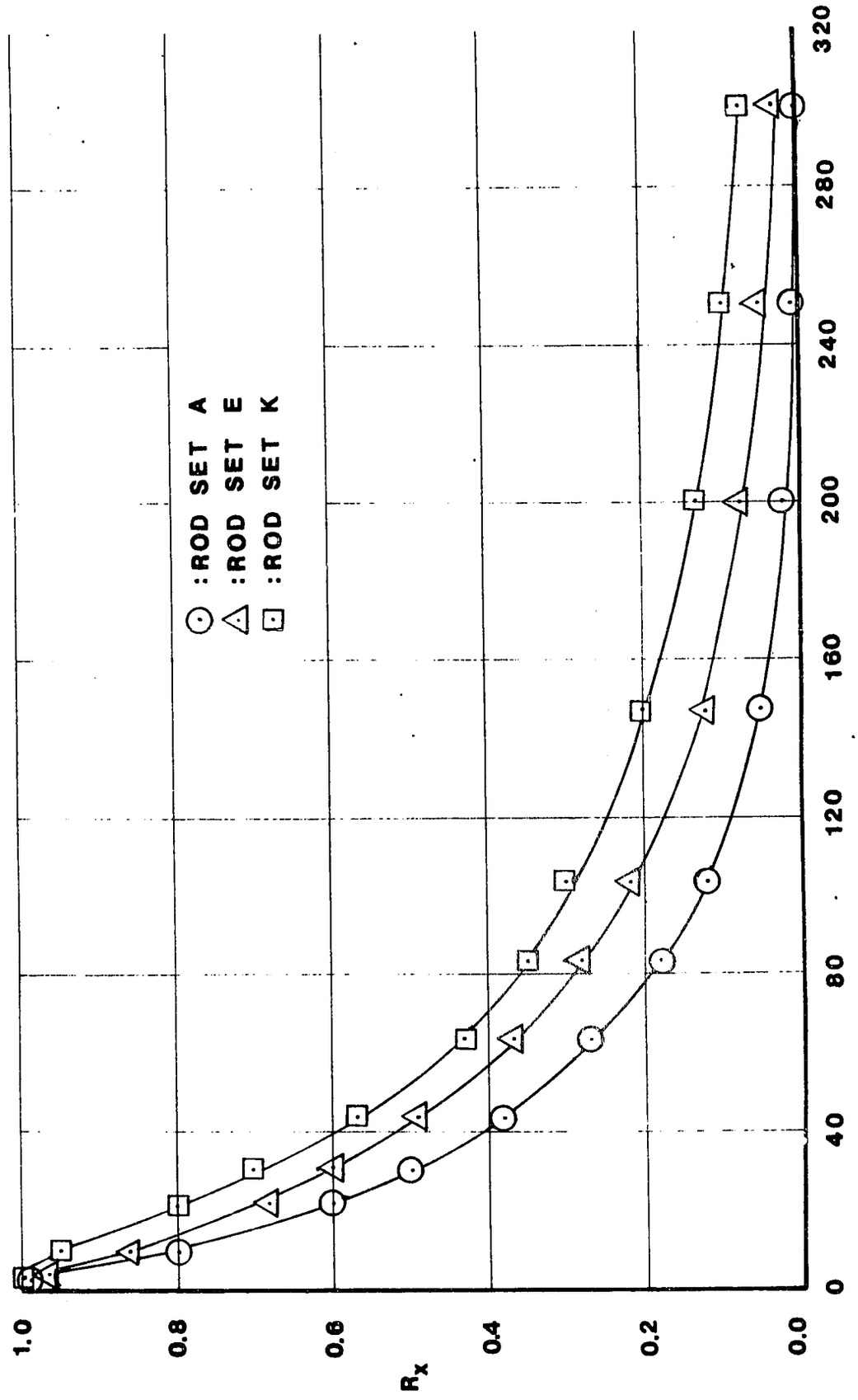

Figure 8

Free-Stream Correlation Coefficient vs Time Delay Curves

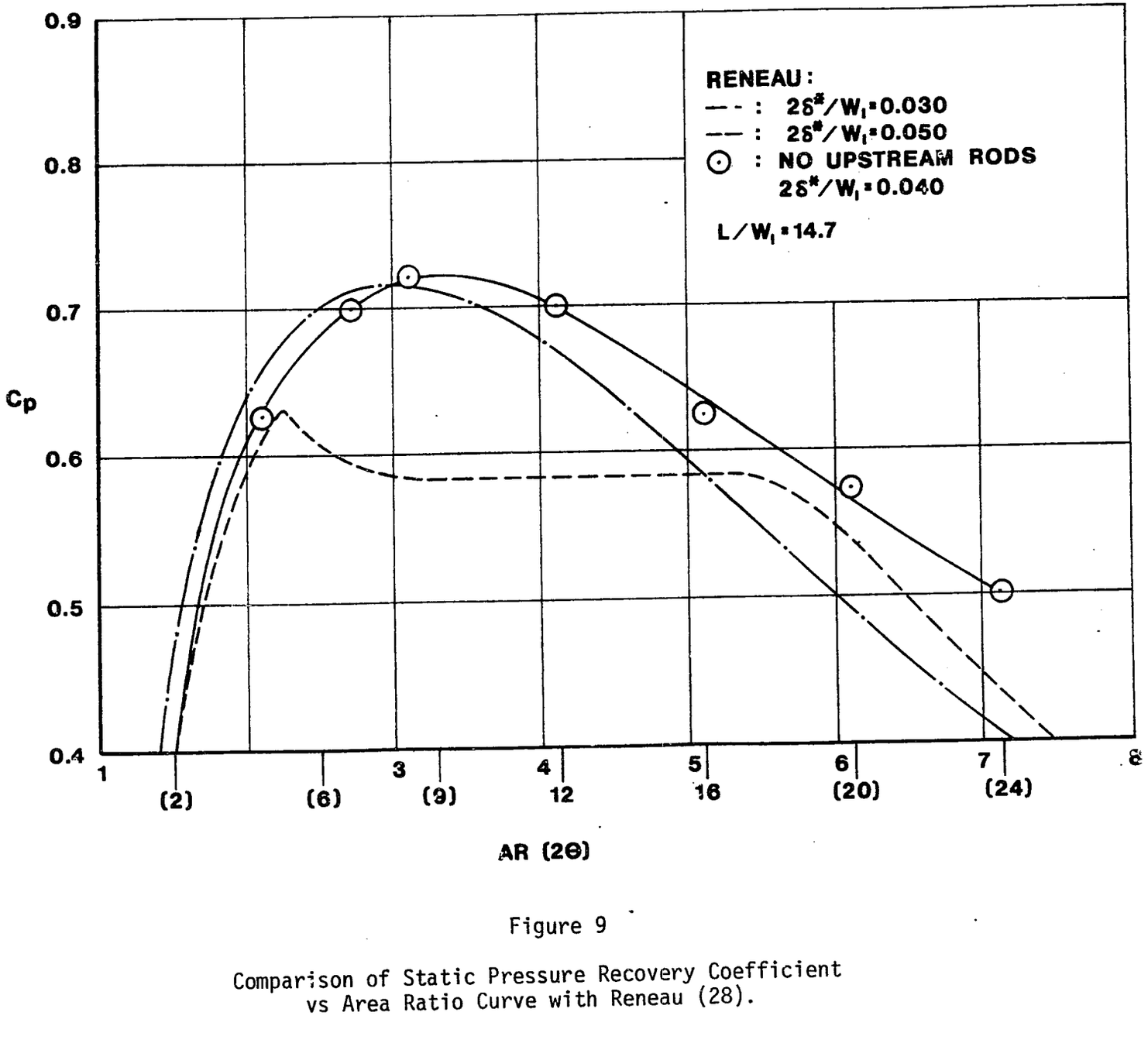

Figure 9

Comparison of Static Pressure Recovery Coefficient vs Area Ratio Curve with Reneau (28).

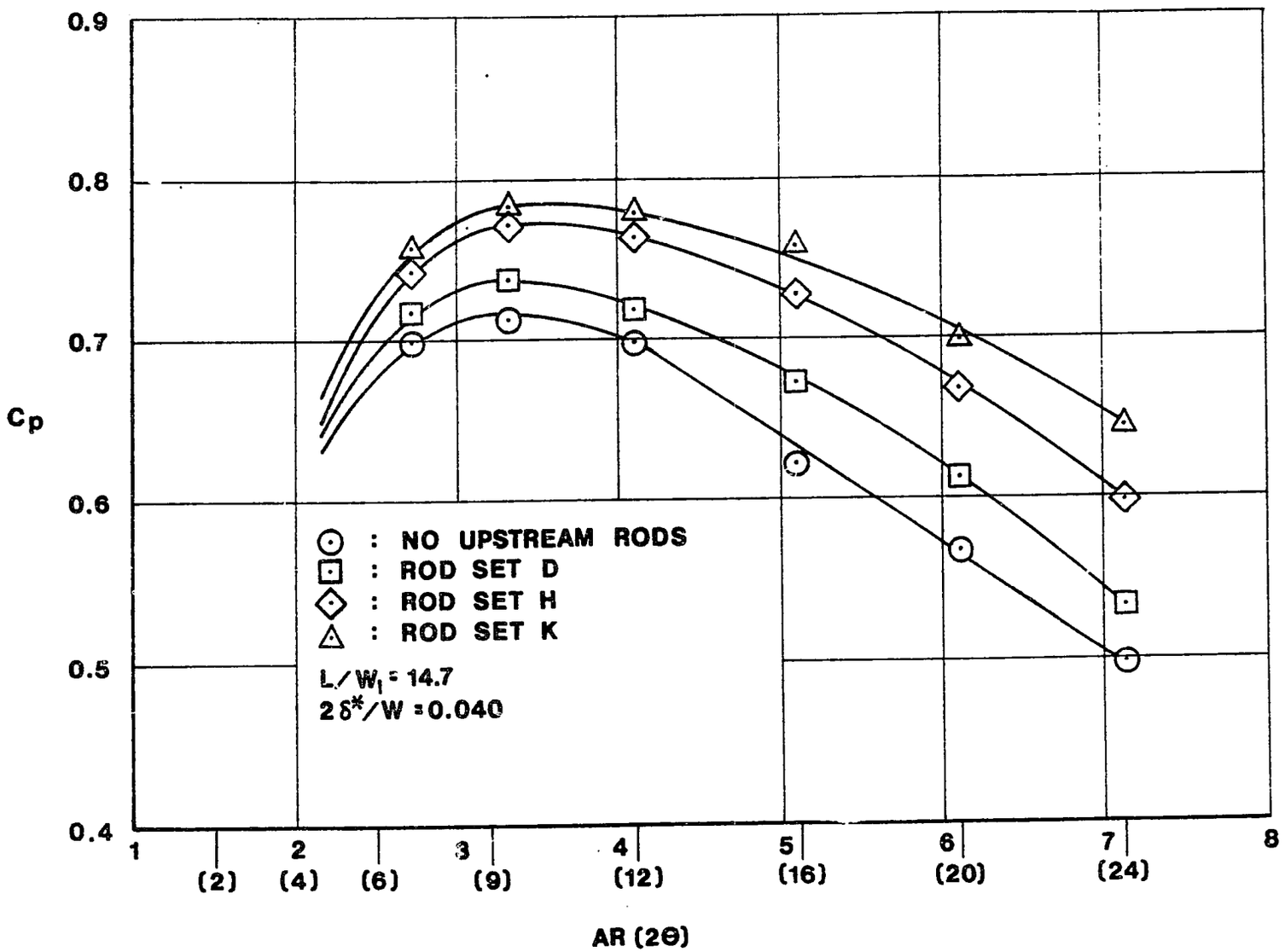

Figure 10a

Static Pressure Recovery Coefficient vs Area Ratio Curves

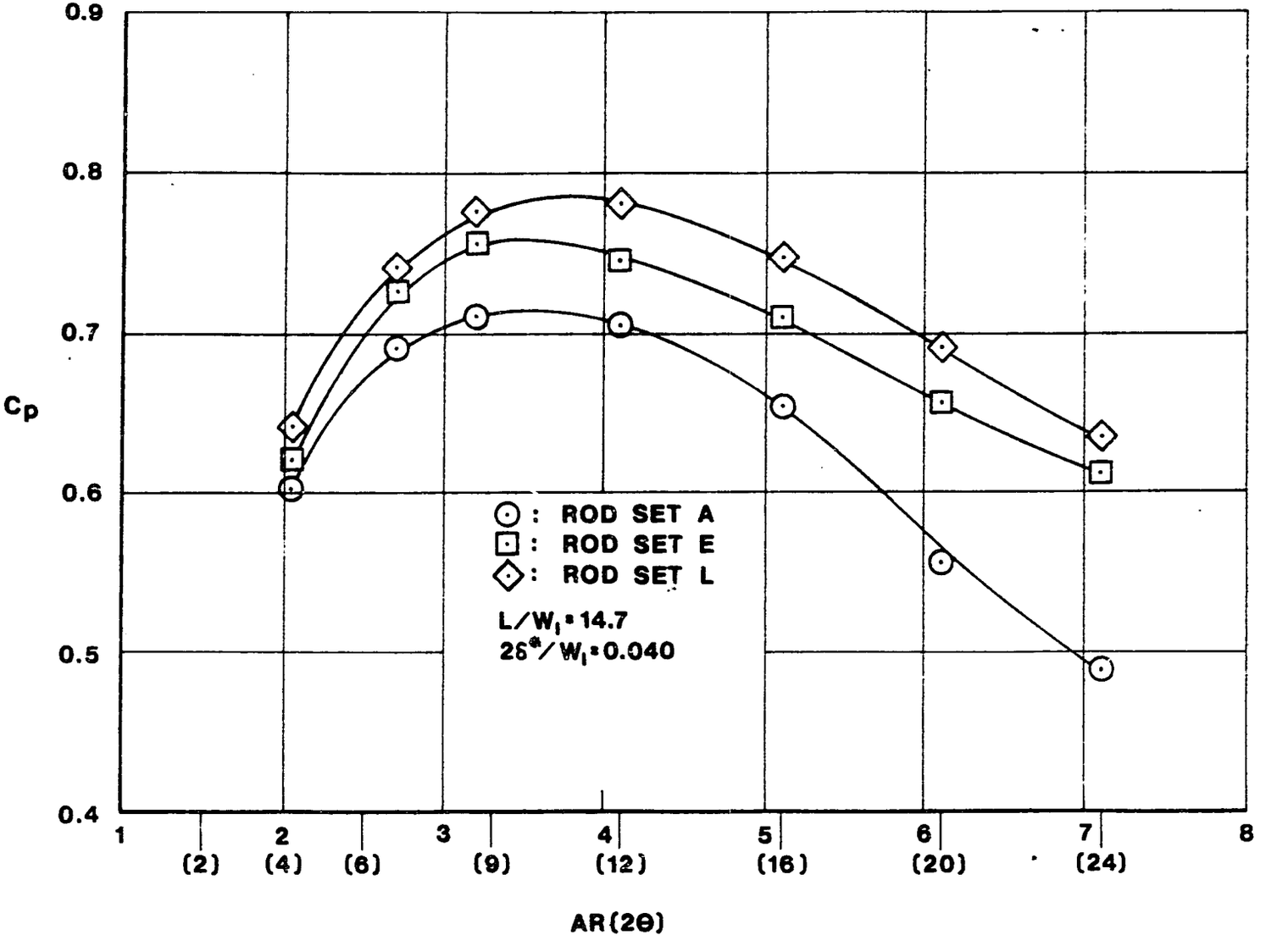

Figure 10b

Static Pressure Recovery Coefficient vs Area Ratio Curves

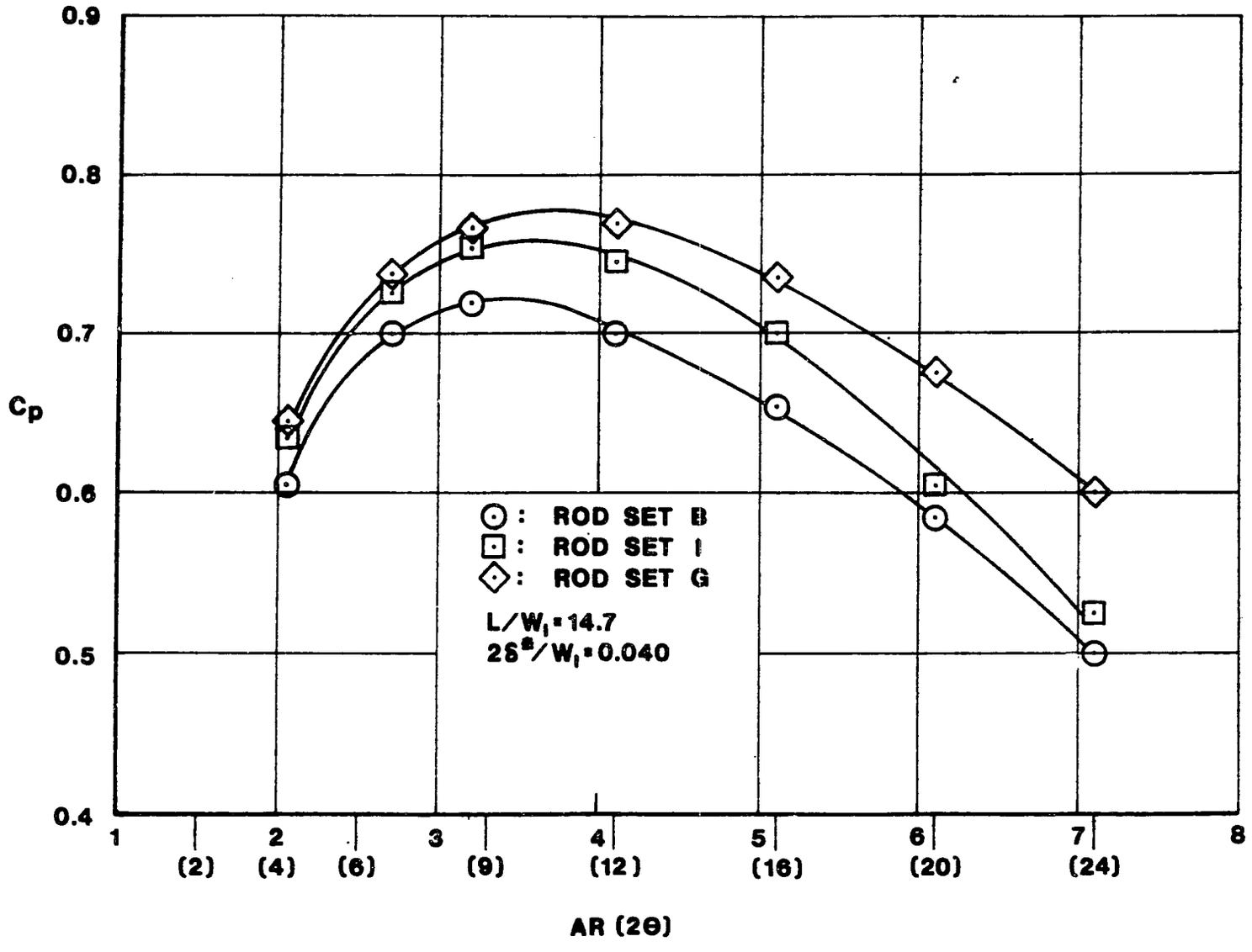

Figure 10c

Static Pressure Recovery Coefficient vs Area Ratio Curves

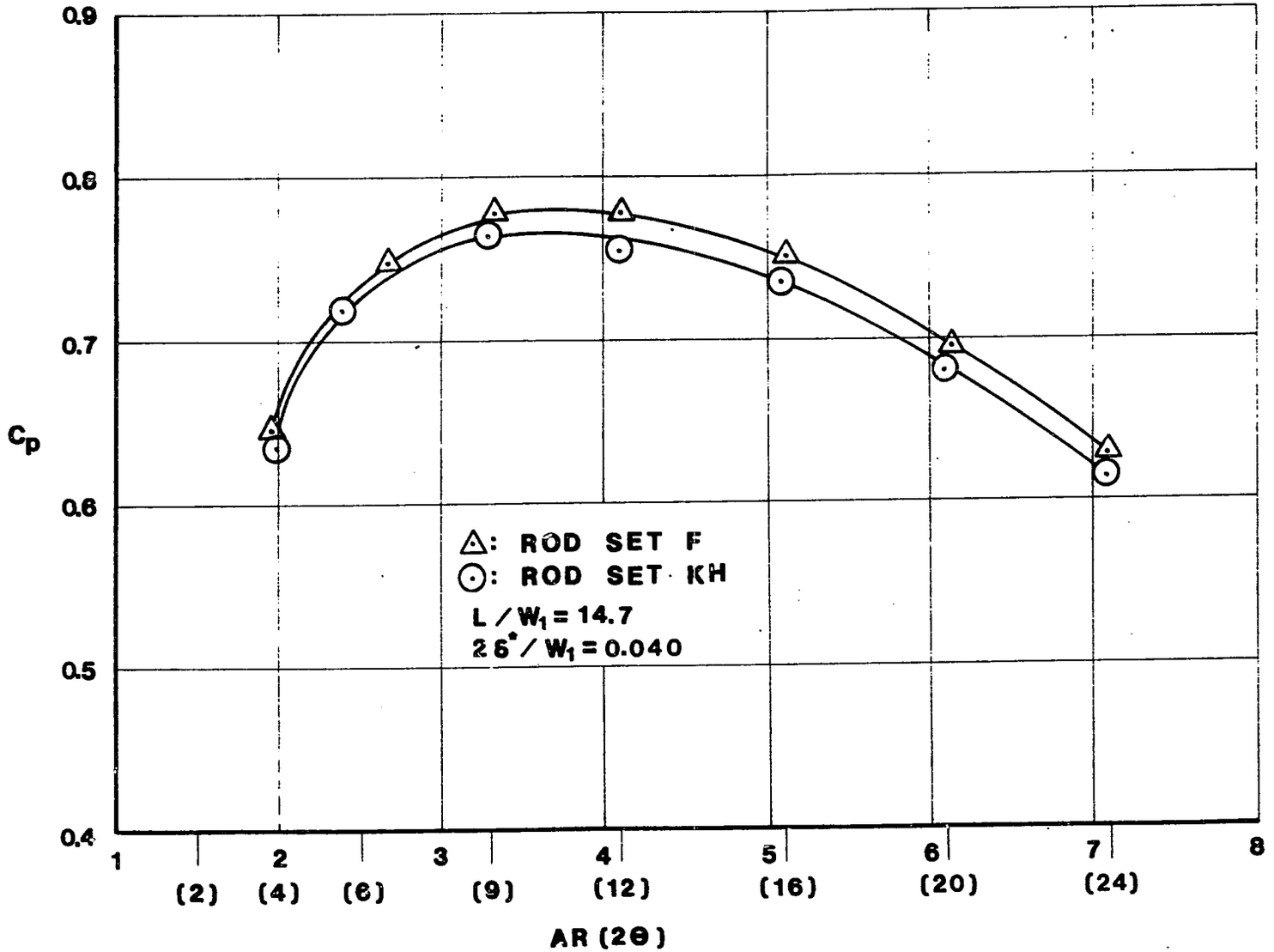

Figure 10d

Static Pressure Recovery Coefficient vs Area Ratio Curves

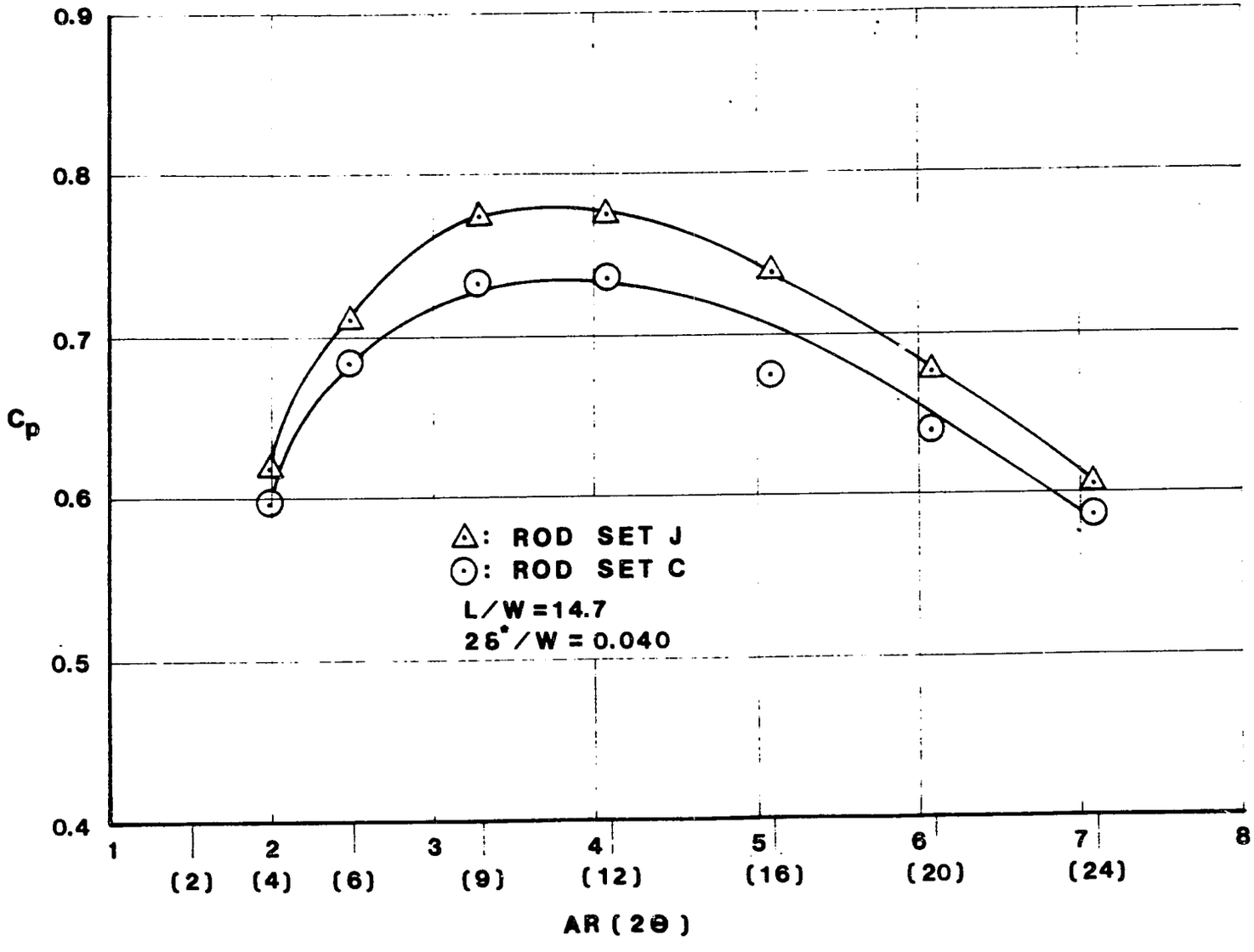

Figure 10e

Static Pressure Recovery Coefficient vs Area Ratio Curves

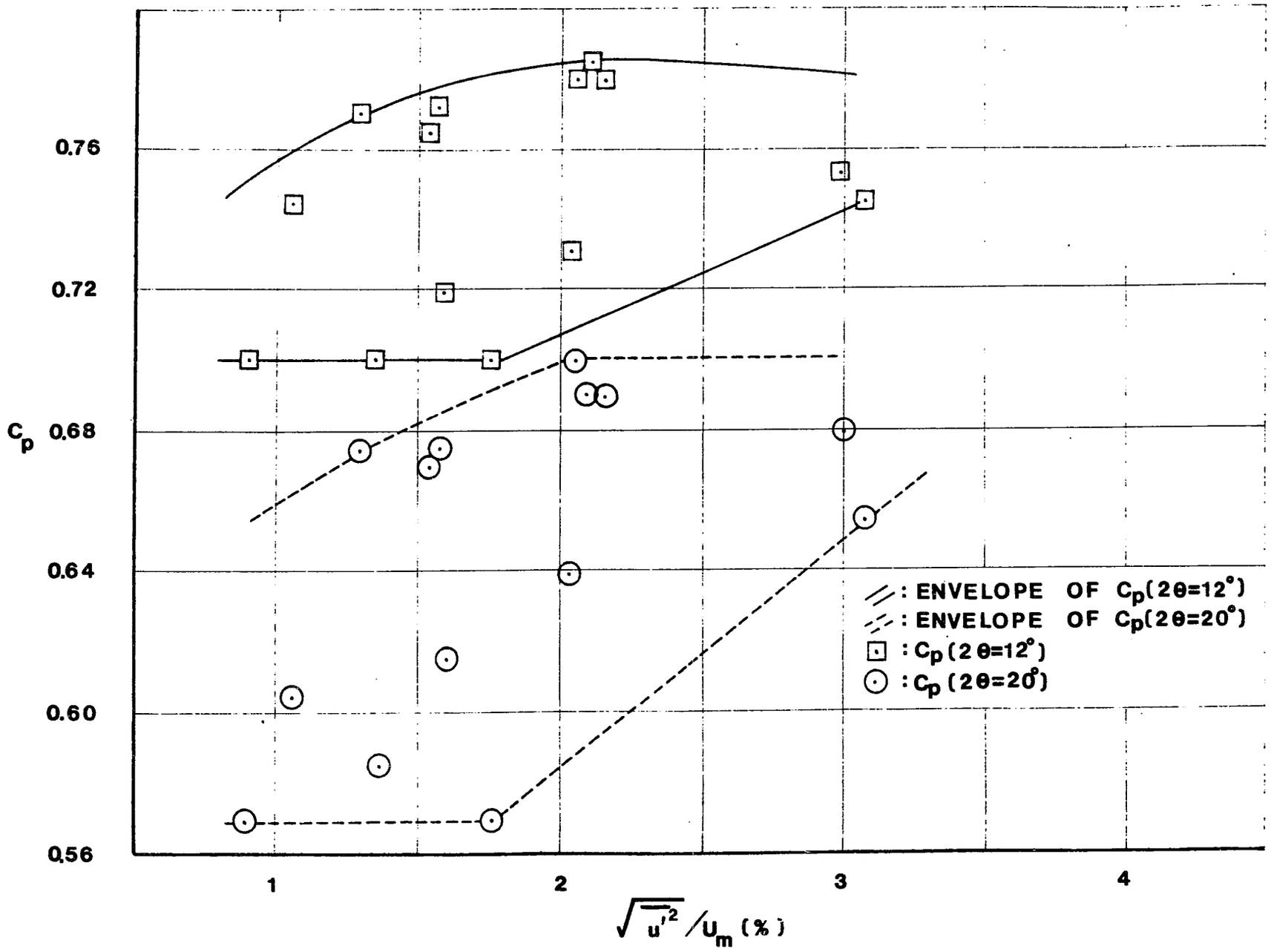

Figure 11
Static Pressure Recovery Coefficient vs Inlet Free-Stream Longitudinal Turbulence Intensity

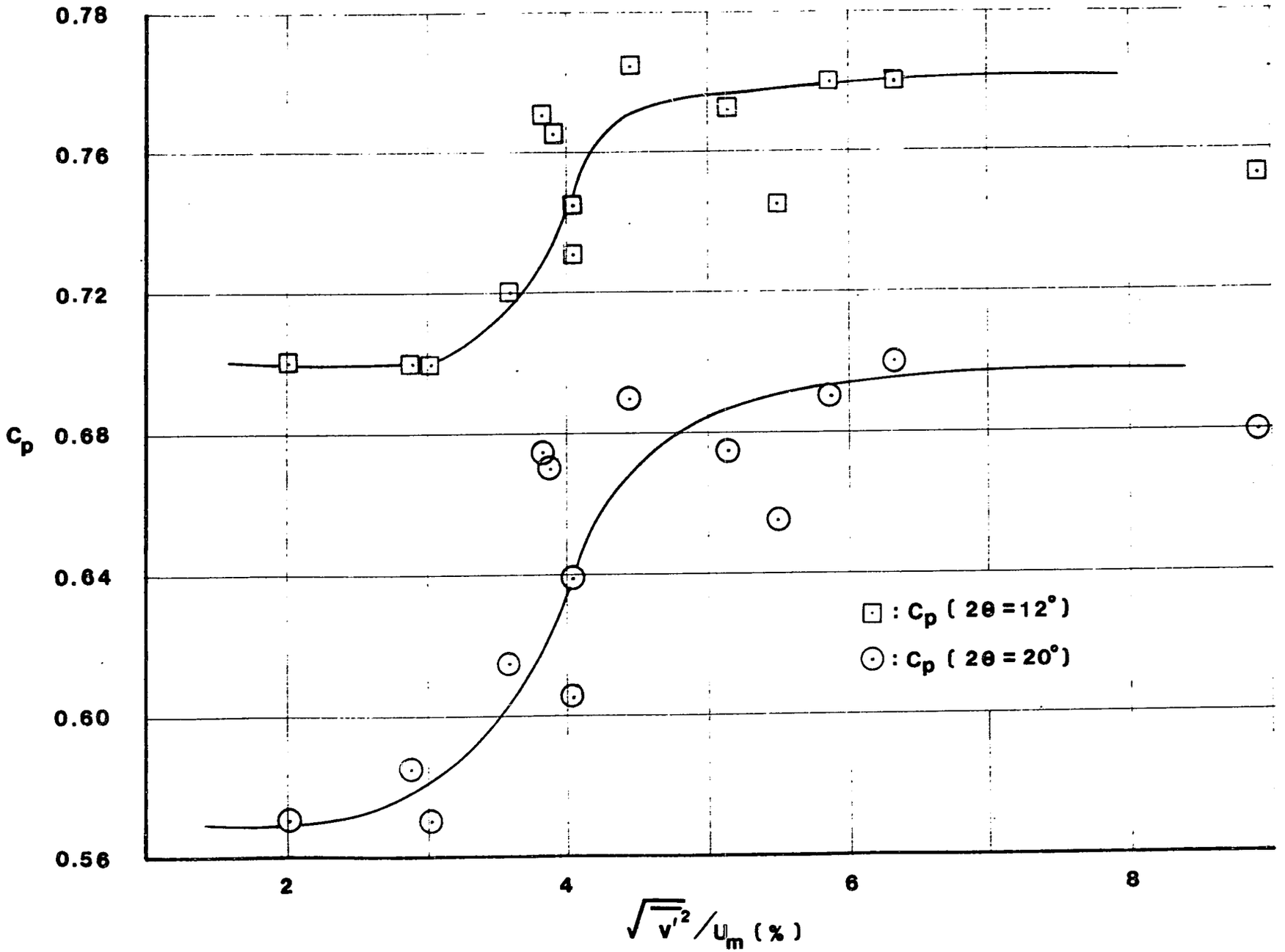

Figure 12

Static Pressure Recovery Coefficient vs Inlet Free-Stream Turbulence Intensity in y Direction

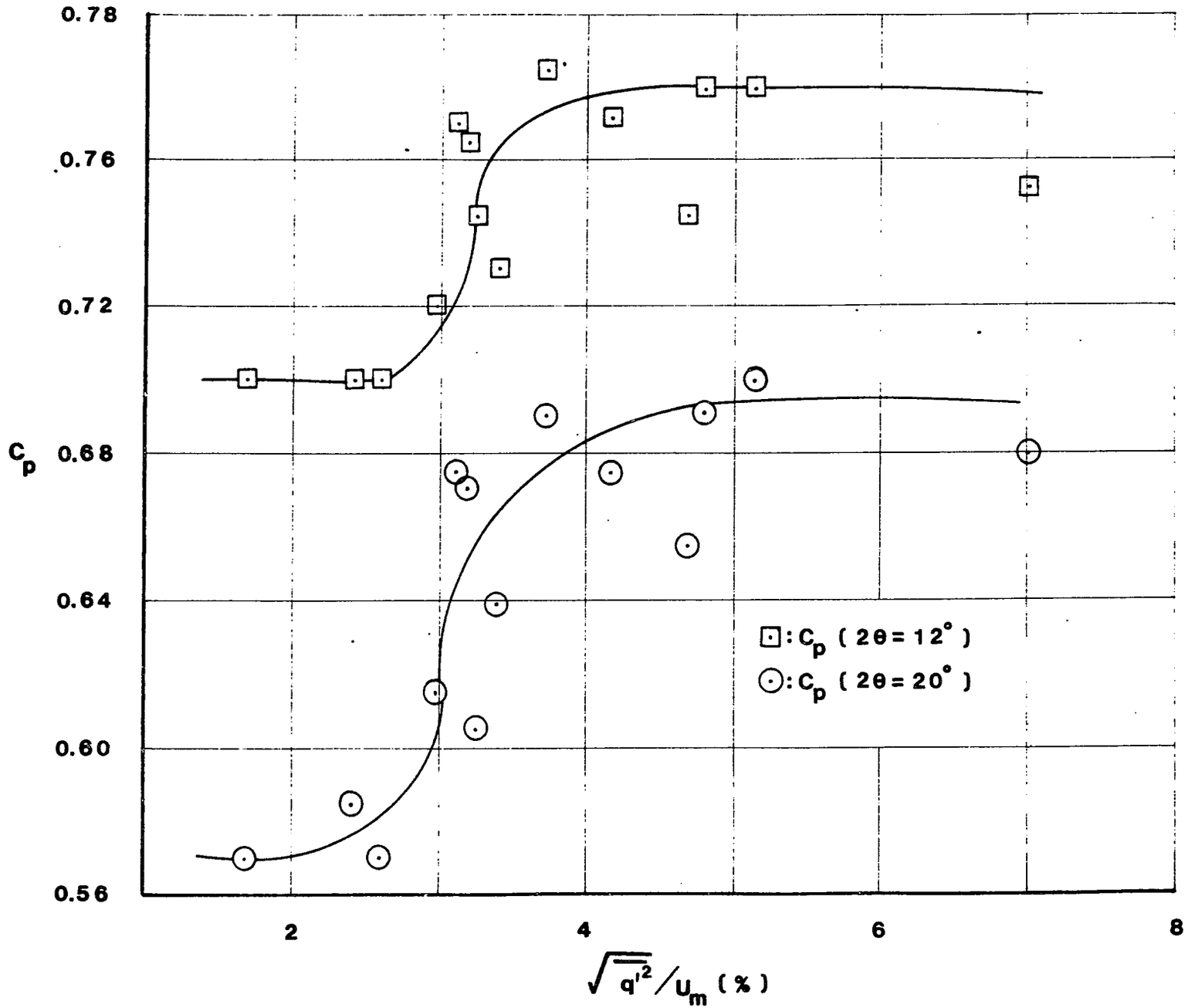

Figure 13

Static Pressure Recovery Coefficient vs Inlet Free-Stream Total Turbulence Intensity

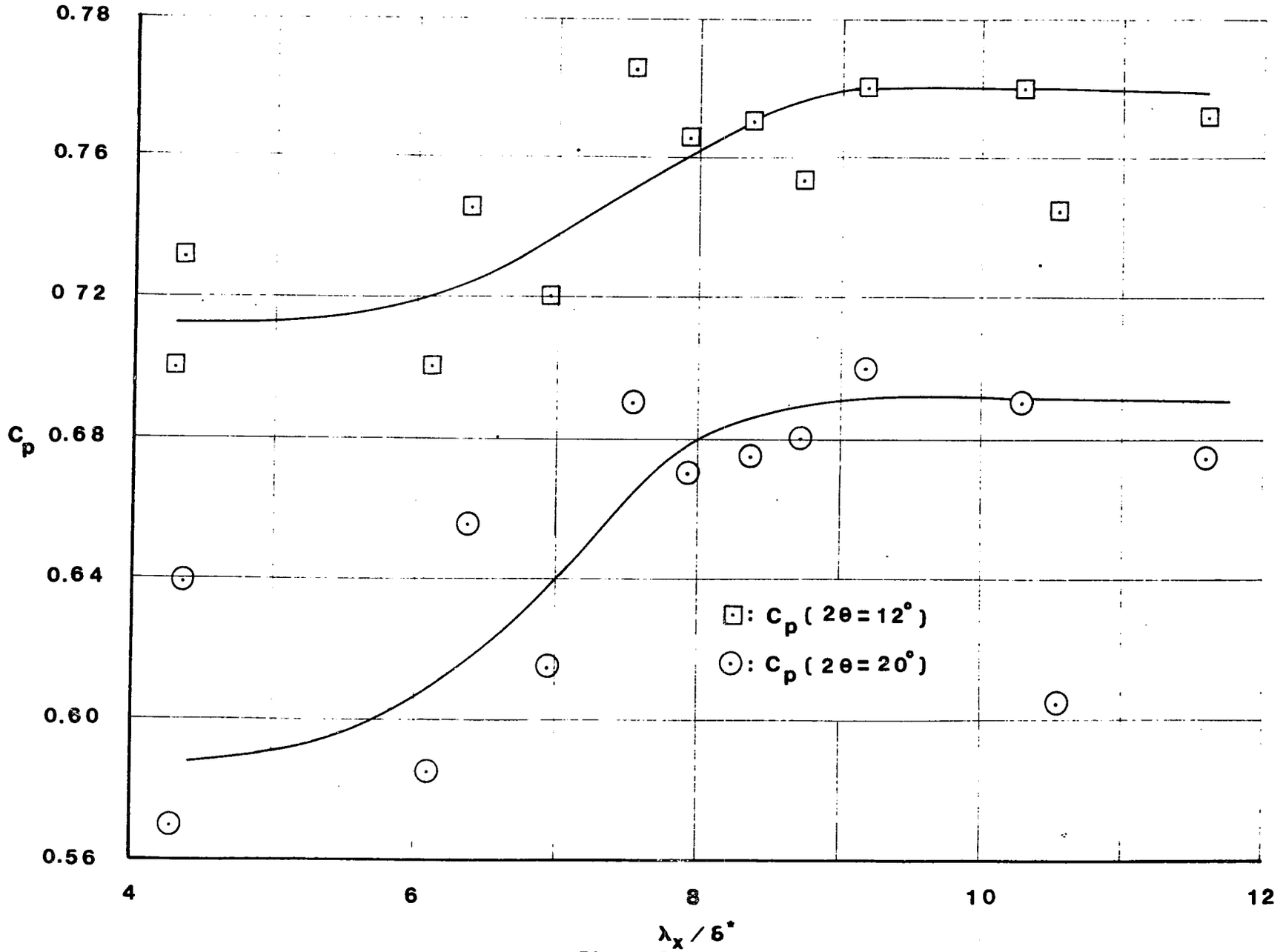

Figure 14

Static Pressure Recovery Coefficient vs Inlet Free-Stream
Integral Scale of Turbulence in Flow Direction

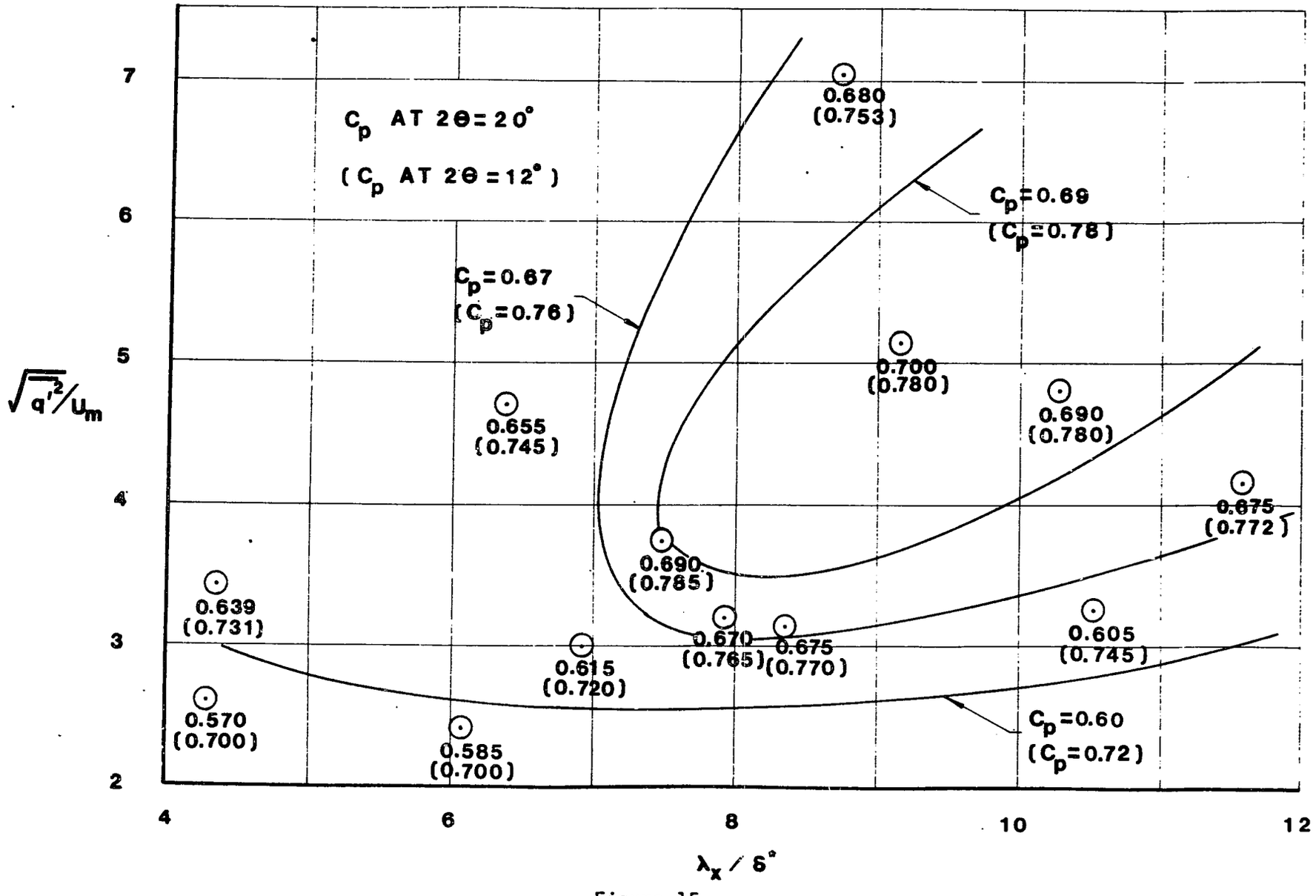

Figure 15

Inlet Free-Stream Total Turbulence Intensity vs Inlet Free-Stream Dimensionless Integral Scale of Turbulence with Static Pressure Recovery Coefficient Contours